One-meson radiative tau decays

Zhi-Hui Guo[1] and Pablo Roig[2]

[1]*CAFPE and Departamento de Física Teórica y del Cosmos, Universidad de Granada,*
Campus de Fuente Nueva, E-18002 Granada, Spain
[2]*Laboratoire de Physique Théorique (UMR 8627), Université de Paris-Sud XI, Bâtiment 210, 91405 Orsay cedex, France*

We have studied the one-meson radiative tau decays $\tau^- \to \nu_\tau \pi^- (K^-) \gamma$, computing the structure-dependent contributions within a Lagrangian approach based on the large-N_C limit of QCD that ensures the proper low-energy limit dictated by chiral symmetry. Upon imposing the short-distance QCD constraints to the form factors, we are able to predict the structure-dependent radiation without any free parameter and, therefore, the relevant observables for the decay $\tau^- \to \nu_\tau \pi^- \gamma$: the photon energy spectrum, the invariant mass spectrum of the meson-photon system, and the integrated decay rate. We also discuss the remaining uncertainties in these observables for the $\tau^- \to \nu_\tau K^- \gamma$ decay. According to our results, the present facilities could detect these rare decays for the first time in the near future, allowing for a stringent test of our predictions.

I. INTRODUCTION

The decays of the τ lepton are an ideal benchmark to analyze the hadronization of the spin-one QCD currents and to learn about the treatment of the strong interaction involving the intermediate meson dynamics in rather clean conditions, since the electroweak part of the decay is under good theoretical control and the light-flavored hadron resonances rule these processes [1–12].

Among the various exclusive tau decays, we are in this article particularly interested in the one-meson radiative tau decays, i.e., $\tau \to \pi(K)\nu\gamma$. Unlike in many of the multi-pseudoscalar tau decay channels, where the excited vector resonances (such as ρ', $K^{*\prime}$) could play a significant role due to the kinematics effects, the channels we are going to study here should be less influenced by the excited resonances, since the lowest vector resonances, such as $\rho(770)$, $K^*(892)$, could already decay into $\pi(K)\gamma$ at their on-shell energy regions. So these radiative decay processes can provide us with an excellent environment to investigate the lowest resonance states. On the experimental side, these channels have not been detected yet, which makes our analysis more meaningful since the current work could serve as a helpful tool for the measurements of these channels in the B- and tau-charm factories in the near future.

The decay amplitude for the one-meson radiative decay of the τ includes an internal bremsstrahlung (IB) component, that is given by QED, and thus can be calculated unambiguously to any desired order in perturbation theory. In addition, one has the structure-dependent (SD) part, dominated by the effects of the strong interaction. Lorentz symmetry determines that there are two independent structures, the so-called vector and axial-vector form factors that encode our lack of knowledge of the precise mechanism responsible for hadronization.

One then has to rely on parametrizations of these form factors. Some of the earliest attempts can be found in Ref. [1]. The so-called Kühn-Santamaría model [6] became a very popular approach. For a given meson mode it proceeds as follows: It normalizes the form factor using the lowest order contribution stemming from the low-energy effective field theory of QCD in the light-flavored sector: chiral perturbation theory, χPT [13–16]. Then the form factor is constructed in terms of Breit-Wigner functions weighted by some unknown parameters (to be fitted to data) in such a way that it vanishes at infinite transfer of momentum in order to obey a Brodsky-Lepage behavior [17,18]. This procedure was used successfully to describe the ARGUS data on the $\tau \to \pi\pi\pi\nu_\tau$ decays [19]. However, as the data became more precise [20], it was shown that there was room for improvement [8,12]. Among the theoretical reasons for this, one finds that in the low-energy limit this model is not consistent with χPT at $\mathcal{O}(p^4)$ [8,21]. Assorted versions of the Kühn-Santamaría model have been used for several two- and three-meson tau decays [3,22] and also for the radiative one-meson decays we consider in this article [4]. In general, these works made following Ref. [6] suffer from additional problems, as discussed in Ref. [23]. In fact, arbitrary parametrizations are of little help in order to comprehend the characteristics of the hadronization procedure independently of their eventual success in describing experimental data. The best procedure in order to investigate this problem should be to build the relevant form factors upon as many QCD features as possible.

The TAUOLA library [24] is currently the most relevant tool to analyze tau decay data. Although it only incorporated the Kühn-Santamaría models at first, it was enriched with parametrizations by the experimental collaborations ALEPH and CLEO (collected in Ref. [25]) in order to explain their data. In the B-factories era, however, it has

become evident that this strategy is not adequate, and TAUOLA has been opened to the introduction of matrix elements obtained within other approaches that include more properties stemming from QCD. This makes it an excellent tool to exploit the synergies of Monte Carlo methods and theoretical approaches to better understand the large data samples of high quality obtained at the B-factories (BABAR, Belle) and the τ-charm factories, such as BES-III. This is thus an appropriate benchmark where the results of our research can be applied.

Although one knows the underlying theory, QCD, this kind of study is rather involved since there is no fully analytic way of relating the final state mesons that are detected to the quark and gluon degrees of freedom of the QCD Lagrangian. Moreover we are in the nonperturbative regime of the strong interaction ($E \lesssim M_\tau \sim 1.7$ GeV), so any perturbative treatment within QCD will not be a good approach to the problem.

At very low energies ($E \lesssim M_\rho$, being M_ρ the mass of the $\rho(770)$ resonance), the chiral symmetry of massless QCD rules the construction of an effective field theory that allows a perturbative expansion in momenta (p) and light quark masses (m), as $(p^2, m_\pi^2)/\Lambda_\chi^2$, with $\Lambda_\chi \sim 4\pi F \sim M_\rho$ being the chiral-symmetry breaking scale. m_π is the pion mass and F is its decay constant, with the normalization of $F = 92.4$ MeV. This theory is χPT, that drives the hadronization of QCD currents into the lightest multiplet of pseudoscalar mesons, including π, K, and η particles. This framework was applied to the two- and three-pion tau decays in Ref. [26], and it was checked that it provides a right description of the low-energy data although it was incapable of providing a good parametrization for the rest of the spectrum. This study put forward that whatever structure due to resonance exchange the form factors may have should match the chiral behavior in the limit where χPT applies. As we brought forward before, the Kühn-Santamaría models already fail to fulfill that condition at $\mathcal{O}(p^4)$ in the chiral expansion [8,21].

We shall extend χPT to energies $E \gtrsim M_\rho$, where the expansion parameter of χPT is no longer valid. In fact, it is not known how to develop a dual effective theory of QCD in this region. However, there is a construct that has proven to be useful in this regime, shedding light on the appropriate structure of the Lagrangian theory, that we could use. This is yielded by the large-N_C limit of $SU(N_C)$ QCD [27], which introduces the inverse of the number of colors (three in the real world) as the parameter to build the expansion upon. In our context, it amounts to considering a spectrum of an infinite number of zero-width resonances that interact at tree level through local effective vertices. This frame, as we will see, can be used to establish a starting point in the study of the resonance region and consequently in the hadronic decays of the tau lepton we are dealing with. The setting recalls the rôle of the resonance chiral theory

($R\chi T$) [28,29] that can be better understood in the light of the large-N_C limit of QCD as a theory of hadrons [30,31].

The theory, although built upon symmetries guided by the large-N_C expansion and reproducing the chiral behavior in the low-energy region, is still missing an ingredient of QCD. At higher energies ($E \gg M_\rho$), where the light-flavored continuum is reached, perturbative QCD is the appropriate tool to deal with the description of interactions, which is given in terms of partons. A well-known feature of form factors of QCD currents is their smooth behavior at high energies [17,18]. Then it is plausible that the form factors match this behavior above the energy region where the resonances lie. A complementary approach is given by the study of the operator product expansion (OPE) of Green functions of QCD currents that are order parameters of the chiral symmetry breakdown. Refs. [32–37] have evaluated these Green functions within a resonance theory and proceeded to match the outcome to the leading term of the OPE at high transfers of momenta. As we commented earlier, it is crucial to take into account this high-energy information to settle a resonance Lagrangian that implements as many QCD features as possible, whence the described procedure will help to establish relations among some of the Lagrangian couplings, and eventually fix others [37].

We will consider the SD description of the processes $\tau^- \to P^- \gamma \nu_\tau$ ($P = \pi, K$) within the framework of $R\chi T$ as introduced in this section and discussed in detail in the following section. These channels have not been observed yet, which is strange according to the most naïve expectations of their decay rates. Clarifying this question is one of the main motivations of our study.

The relative sign between the IB- and SD-dependent parts motivated an addendum to Ref. [4]. This confusion was caused by the fact that they did not use a Lagrangian approach. In any such approach this should not be an issue. In order to facilitate any independent check, we define the convention we follow as the one used by PDG [38] in order to relate the external fields r_μ, l_μ with the physical photon field

$$r_\mu = l_\mu = -eQA_\mu, \qquad (1)$$

where e is the electric charge of the positron and the charge matrix of the three light-flavor quarks is $Q = \text{diag}(\frac{2}{3}, -\frac{1}{3}, -\frac{1}{3})$. Determining the relative sign between the structure-independent (SI) and dependent contributions is an added interest of our computation.

The SI part of the process has been discussed in [4]. We will compute the SD part using the Lagrangians in Sec. II. The kinematics and differential decay rates are discussed in Sec. III, as well as the general form of the matrix elements and the spectra. The structure-dependent form factors for each mode are computed in Secs. IV and V. The QCD short-distance constraints are presented in Sec. VI, and the phenomenological implications are detailed in

Sec. VII. Finally, we summarize and discuss our results in Sec. VIII.

II. THEORETICAL FRAMEWORK

The hadronization of the currents that rule semileptonic tau decays is driven by nonperturbative QCD. As mentioned in the Introduction, our methodology stands on the construction of an action, with the relevant degrees of freedom, led by the chiral symmetry and the known asymptotic behavior of the form factors and Green functions driven by large N_C QCD. We will present here those pieces of the action that are relevant for the study of one-meson radiative decays of the tau lepton. Hence we will need to include both even- and odd-intrinsic-parity sectors.

The large N_C expansion of $SU(N_C)$ QCD implies that, in the $N_C \to \infty$ limit, the study of Green functions of QCD currents and associated form factors can be carried out through the tree-level diagrams of a Lagrangian theory that includes an infinite spectrum of strictly stable states [27].[1] Therefore the study of the resonance energy region can be performed by constructing such a Lagrangian theory. However, it is not known how to implement an infinite spectrum in a model-independent way. Moreover, it is well known from the phenomenology that the main role is always played by the lightest resonances. Accordingly, it was suggested in Refs. [28,29] that one can construct a suitable effective Lagrangian involving the lightest multiplets of resonances and the pseudo-Goldstone bosons (π, K, and η). This is indeed an appropriate tool to handle the hadronic decays of the tau lepton and the pion form factors [8–12,40–42]. The guiding principle in the construction of such a Lagrangian is chiral symmetry. When resonances are integrated out from the theory, i.e., when one tries to describe the energy region below such states ($E \ll M_\rho$), the remaining setting is χPT, reviewed in Refs. [43,44].

The very low-energy strong interaction in the light quark sector is known to be ruled by the $SU(3)_L \otimes SU(3)_R$ chiral symmetry of massless QCD implemented in χPT. The leading even-intrinsic-parity $\mathcal{O}(p^2)$ Lagrangian, which carries the information of the spontaneous symmetry breaking of the theory, is:

$$\mathcal{L}_{\chi\text{PT}}^{(2)} = \frac{F^2}{4} \langle u_\mu u^\mu + \chi_+ \rangle, \qquad (2)$$

where

$$\begin{aligned} u_\mu &= i[u^\dagger(\partial_\mu - ir_\mu)u - u(\partial_\mu - i\ell_\mu)u^\dagger], \\ \chi_\pm &= u^\dagger \chi u^\dagger \pm u\chi^\dagger u, \qquad \chi = 2B_0(s + ip), \end{aligned} \qquad (3)$$

----

[1] Since light resonances reach their on-shell peaks in the energy region spanned by the considered decays, the corresponding off-shell widths, which are energy-dependent, need to be implemented as we do, following Refs. [12,39].

and $\langle \dots \rangle$ is short for the trace in the flavor space. The Goldstone octet of pseudoscalar fields,

$$\Phi(x) = \begin{pmatrix} \frac{1}{\sqrt{2}}\pi^0 + \frac{1}{\sqrt{6}}\eta_8 & \pi^+ & K^+ \\ \pi^- & -\frac{1}{\sqrt{2}}\pi^0 + \frac{1}{\sqrt{6}}\eta_8 & K^0 \\ K^- & \bar{K}^0 & -\frac{2}{\sqrt{6}}\eta_8 \end{pmatrix},$$

$$(4)$$

is realized nonlinearly into the unitary matrix in the flavor space

$$u(\varphi) = \exp\left\{\frac{i}{\sqrt{2}F}\Phi(x)\right\}, \qquad (5)$$

which under chiral rotations transforms as

$$u(\varphi) \to g_R u(\varphi)h(g, \varphi)^\dagger = h(g, \varphi)u(\varphi)g_L^\dagger, \qquad (6)$$

with $g \equiv (g_L, g_R) \in SU(3)_L \otimes SU(3)_R$ and $h(g, \varphi) \in SU(3)_V$. External hermitian matrix fields r_μ, l_μ, s, and p promote the global $SU(3)_L \otimes SU(3)_R$ symmetry to a local one. Thus, interactions with electroweak bosons can be accommodated through the vector $v_\mu = (r_\mu + l_\mu)/2$ and axial-vector $a_\mu = (r_\mu - l_\mu)/2$ fields. The scalar field s incorporates the explicit chiral symmetry breaking through the quark masses taking $s = \mathcal{M} + \dots$, with $\mathcal{M} = \text{diag}(m_u, m_d, m_s)$, where we will always work in the isospin limit in the present discussion, i.e., $m_u = m_d$. Finally, at lowest order in the chiral expansion, F is the pion decay constant and $B_0 F^2 = -\langle \bar{\psi}\psi \rangle$, with the quark condensate $\langle \bar{\psi}\psi \rangle = \langle \bar{u}u \rangle = \langle \bar{d}d \rangle = \langle \bar{s}s \rangle$.

The leading action in the odd-intrinsic-parity sector arises at $\mathcal{O}(p^4)$. This is given by the chiral anomaly [45] and explicitly stated by the Wess-Zumino-Witten (WZW) functional $\mathcal{Z}_{WZW}[v, a]$ that can be read in Ref. [43]. This contains all anomalous contributions to electromagnetic and semileptonic meson decays. For completeness, we give the relevant terms to $\tau \to P\gamma\nu_\tau$ below:

$$\begin{aligned} \mathcal{L}_{WZW} &= -\frac{iN_C}{48\pi^2}\varepsilon_{\mu\nu\alpha\beta}\langle \Sigma_L^\mu U^\dagger \partial^\nu r^\alpha U l^\beta + \Sigma_L^\mu l^\nu \partial^\alpha l^\beta \\ &+ \Sigma_L^\mu \partial^\nu l^\alpha l^\beta - (L \leftrightarrow R) \rangle, \end{aligned} \qquad (7)$$

with $U = u^2$, $\Sigma_L^\mu = U^\dagger \partial^\mu U$ and $\Sigma_R^\mu = U\partial^\mu U^\dagger$.

It is well known [28,46] that higher orders in the chiral expansion, i.e., even-intrinsic-parity $\mathcal{L}_{\chi\text{PT}}^{(n)}$ with $n > 2$, bring in the information of heavier degrees of freedom that have been integrated out, for instance, resonance states. As our next step intends to include the latter explicitly, we will not consider higher orders in χPT in order to avoid double-counting issues. In order to fulfill this procedure—at least, up to $\mathcal{O}(p^4)$ in the even-intrinsic-parity sector—it is convenient to use the antisymmetric tensor representation for the $J = 1$ fields, as we mention below. Analogously, additional odd-intrinsic-parity amplitudes

arise at $\mathcal{O}(p^6)$ in χPT, either from one-loop diagrams using one vertex from the *WZW* action or from tree-level operators [47]. However, we will assume that the latter are fully generated by resonance contributions [34] and, therefore, will not be included in the following discussion.

The formulation of a Lagrangian theory that includes both the octet of Goldstone mesons and $U(3)$ nonets of resonances is carried out through the construction of a phenomenological Lagrangian [48] where chiral and discrete symmetries determine the structure of the operators. Given the vector character of the standard model (SM) couplings of the hadron matrix elements in τ decays, form factors for these processes are ruled by vector and axial-vector resonances. Notwithstanding, those form factors are given, in the $\tau \to P\gamma\nu_\tau$ decays, by a three-point Green function where other quantum numbers might play a role, namely, scalar and pseudoscalar resonances [49]. However their contribution should be very small for $\tau \to P\gamma\nu_\tau$. This statement is based on the following observations: The scalar resonances will be irrelevant at tree level to the considered process due to the discrete symmetry; about the pseudoscalar resonances, their contributions are suppressed due first to their heavy masses and also to the fact that the relevant couplings involving the pseudoscalar resonances should be very tiny, since the decay of these states to $P\gamma$ has not been reported yet. Thus in our description we include $J = 1$ resonances only, and this is done by considering a nonet of fields [28]:

$$R \equiv \frac{1}{\sqrt{2}} \sum_{i=0}^{8} \lambda_i \phi_{R,i}, \tag{8}$$

where $R = V, A$, stand for the vector and axial-vector resonance states. Under the $SU(3)_L \otimes SU(3)_R$ chiral group, R transforms as:

$$R \to h(g, \varphi) R h(g, \varphi)^\dagger. \tag{9}$$

The flavor structure of the resonances is analogous to that of the Goldstone bosons in Eq. (4). One can also introduce the covariant derivative

$$\begin{aligned}
\nabla_\mu X &\equiv \partial_\mu X + [\Gamma_\mu, X], \\
\Gamma_\mu &= \frac{1}{2}[u^\dagger(\partial_\mu - ir_\mu)u + u(\partial_\mu - i\ell_\mu)u^\dagger],
\end{aligned} \tag{10}$$

acting on any object X that transforms as R in Eq. (9), like u_μ and $\chi_\pm$. The kinetic terms for the spin-one resonances in the Lagrangian read [28]:

$$\mathcal{L}_{\text{kin}}^R = -\frac{1}{2}\langle \nabla^\lambda R_{\lambda\mu} \nabla_\nu R^{\nu\mu}\rangle + \frac{M_R^2}{4}\langle R_{\mu\nu} R^{\mu\nu}\rangle, \quad R = V, A, \tag{11}$$

M_V, M_A being the masses of the nonets of vector and axial-vector resonances in the chiral and large-N_C limits, respectively. Notice that we describe the resonance fields through the antisymmetric tensor representation. With this description

tion one is able to collect, upon integration of the resonances, the bulk of the low-energy couplings at $\mathcal{O}(p^4)$ in χPT without the inclusion of additional local terms [37]. So it is necessary to use this representation if one does not include $\mathcal{L}_{\chi\text{PT}}^{(4)}$ in the Lagrangian. Though analogous studies at higher chiral orders have not been carried out, we will assume that no $\mathcal{L}_{\chi\text{PT}}^{(n)}$ with $n = 4, 6, \ldots$ in the even-intrinsic-parity and $n = 6, 8, \ldots$ in the odd-intrinsic-parity sectors need to be included in the theory.

The construction of the interaction terms involving resonance and Goldstone fields is driven by chiral and discrete symmetries with a generic structure given by

$$\mathcal{O}_i \sim \langle R_1 R_2 \ldots R_j \chi^{(n)}(\varphi)\rangle, \tag{12}$$

where $\chi^{(n)}(\varphi)$ is a chiral tensor that includes only Goldstone and auxiliary fields. It transforms like R in Eq. (9) and has chiral counting n in the frame of χPT. This counting is relevant in the setting of the theory because, although the resonance theory itself has no perturbative expansion, higher values of n may originate violations of the proper asymptotic behavior of form factors or Green functions. As a guide we will include at least those operators that, contributing to our processes, are leading when integrating out the resonances. In addition we do not include operators with higher-order chiral tensors, $\chi^{(n)}(\varphi)$, that would violate the QCD asymptotic behavior unless their couplings are severely fine tuned to ensure the needed cancellations of large momenta. In the odd-intrinsic-parity sector, which contributes to the vector form factor, this amounts to include all $\langle R\chi^{(4)}\rangle$ and $\langle RR\chi^{(2)}\rangle$ terms. In the even-intrinsic-parity sector, contributing to the axial-vector form factors, these are the terms $\langle R\chi^{(2)}\rangle$. However previous analyses of the axial-vector contributions [8,11,12,35] show the relevant role of the $\langle RR\chi^{(2)}\rangle$ terms that, accordingly, are also considered here.

We also assume exact $SU(3)$ symmetry in the construction of the interacting terms, i.e., at the level of couplings. Deviations from exact symmetry in hadronic tau decays have been considered in Ref. [50]. However, we do not include $SU(3)$-breaking couplings because we are not considering next-to-leading order corrections in the $1/N_C$ expansion, either.

The lowest-order interaction operators, linear in the resonance fields, have the structure $\langle R\chi^{(2)}(\varphi)\rangle$. There are no odd-intrinsic-parity terms of this form. The even-intrinsic-parity Lagrangian includes three coupling constants [28]:

$$\begin{aligned}
\mathcal{L}_2^V &= \frac{F_V}{2\sqrt{2}}\langle V_{\mu\nu} f_+^{\mu\nu}\rangle + i\frac{G_V}{\sqrt{2}}\langle V_{\mu\nu} u^\mu u^\nu\rangle, \\
\mathcal{L}_2^A &= \frac{F_A}{2\sqrt{2}}\langle A_{\mu\nu} f_-^{\mu\nu}\rangle,
\end{aligned} \tag{13}$$

where $f_\pm^{\mu\nu} = u F_L^{\mu\nu} u^\dagger \pm u^\dagger F_R^{\mu\nu} u$ and $F_{R,L}^{\mu\nu}$ are the field strength tensors associated with the external right- and left-handed auxiliary fields. All couplings F_V, G_V and F_A are real.

The leading odd-intrinsic-parity operators, linear in the resonance fields, have the form $\langle R\chi^{(4)}(\varphi)\rangle$. We will need those pieces that generate the vertex with one vector resonance, a vector current, and one pseudoscalar. The minimal Lagrangian with these features is:

$$\mathcal{L}_4^V = \sum_{i=1}^{7} \frac{c_i}{M_V} \mathcal{O}_{VJP}^i, \tag{14}$$

where c_i are real dimensionless couplings, and the VJP operators (that is, the vector resonance, vector source, and pseudo-Goldstone boson, respectively) read [34]:

$$\mathcal{O}_{VJP}^1 = \varepsilon_{\mu\nu\rho\sigma}\langle\{V^{\mu\nu}, f_+^{\rho\alpha}\}\nabla_\alpha u^\sigma\rangle,$$
$$\mathcal{O}_{VJP}^2 = \varepsilon_{\mu\nu\rho\sigma}\langle\{V^{\mu\alpha}, f_+^{\rho\sigma}\}\nabla_\alpha u^\nu\rangle,$$
$$\mathcal{O}_{VJP}^3 = i\varepsilon_{\mu\nu\rho\sigma}\langle\{V^{\mu\nu}, f_+^{\rho\sigma}\}\chi_-\rangle,$$
$$\mathcal{O}_{VJP}^4 = i\varepsilon_{\mu\nu\rho\sigma}\langle V^{\mu\nu}[f_-^{\rho\sigma}, \chi_+]\rangle, \tag{15}$$
$$\mathcal{O}_{VJP}^5 = \varepsilon_{\mu\nu\rho\sigma}\langle\{\nabla_\alpha V^{\mu\nu}, f_+^{\rho\alpha}\}u^\sigma\rangle,$$
$$\mathcal{O}_{VJP}^6 = \varepsilon_{\mu\nu\rho\sigma}\langle\{\nabla_\alpha V^{\mu\alpha}, f_+^{\rho\sigma}\}u^\nu\rangle,$$
$$\mathcal{O}_{VJP}^7 = \varepsilon_{\mu\nu\rho\sigma}\langle\{\nabla^\sigma V^{\mu\nu}, f_+^{\rho\alpha}\}u_\alpha\rangle.$$

Notice that we do not include analogous pieces with an axial-vector resonance, that would contribute to the hadronization of the axial-vector current. This has been thoroughly studied in Ref. [8] (see also Ref. [12]) in the description of the $\tau \to \pi\pi\pi\nu_\tau$ process, and it is shown that no $\langle A\chi^{(4)}(\varphi)\rangle$ operators are needed to describe its hadronization. Therefore those operators are not included in our minimal description of the relevant form factors.

In order to study tau decay processes with a pseudoscalar meson and a photon in the final state, one also has to consider nonlinear terms in the resonance fields. Indeed the hadron final state in $\tau \to P\gamma\nu_\tau$ decays can be driven by vertices involving two resonances and a pseudoscalar meson. The structure of the operators that give those vertices is $\langle R_1 R_2 \chi^{(2)}(\varphi)\rangle$ and has been worked out before [8,34]. They include both even- and odd-intrinsic-parity terms:

$$\mathcal{L}_2^{RR} = \sum_{i=1}^{5} \lambda_i \mathcal{O}_{VAP}^i + \sum_{i=1}^{4} d_i \mathcal{O}_{VVP}^i, \tag{16}$$

where λ_i and d_i are unknown real dimensionless couplings. The operators $\mathcal{O}_{RRP}^i$ are given by:

(1) VAP terms

$$\mathcal{O}_{VAP}^1 = \langle[V^{\mu\nu}, A_{\mu\nu}]\chi_-\rangle,$$
$$\mathcal{O}_{VAP}^2 = i\langle[V^{\mu\nu}, A_{\nu\alpha}]h_\mu{}^\alpha\rangle,$$
$$\mathcal{O}_{VAP}^3 = i\langle[\nabla^\mu V_{\mu\nu}, A^{\nu\alpha}]u_\alpha\rangle, \tag{17}$$
$$\mathcal{O}_{VAP}^4 = i\langle[\nabla^\alpha V_{\mu\nu}, A_\alpha{}^\nu]u^\mu\rangle,$$
$$\mathcal{O}_{VAP}^5 = i\langle[\nabla^\alpha V_{\mu\nu}, A^{\mu\nu}]u_\alpha\rangle,$$

with $h_{\mu\nu} = \nabla_\mu u_\nu + \nabla_\nu u_\mu$, and

(2) VVP terms

$$\mathcal{O}_{VVP}^1 = \varepsilon_{\mu\nu\rho\sigma}\langle\{V^{\mu\nu}, V^{\rho\alpha}\}\nabla_\alpha u^\sigma\rangle,$$
$$\mathcal{O}_{VVP}^2 = i\varepsilon_{\mu\nu\rho\sigma}\langle\{V^{\mu\nu}, V^{\rho\alpha}\}\chi_-\rangle,$$
$$\mathcal{O}_{VVP}^3 = \varepsilon_{\mu\nu\rho\sigma}\langle\{\nabla_\alpha V^{\mu\nu}, V^{\rho\alpha}\}u^\sigma\rangle, \tag{18}$$
$$\mathcal{O}_{VVP}^4 = \varepsilon_{\mu\nu\rho\sigma}\langle\{\nabla^\sigma V^{\mu\nu}, V^{\rho\alpha}\}u_\alpha\rangle.$$

We emphasize that $\mathcal{L}_2^{RR}$ is a complete basis for constructing vertices with only one pseudoscalar meson; for a larger number of pseudoscalars, additional operators might be added. As we are only interested in tree-level diagrams, the equation of motion arising from $\mathcal{L}_{\chi PT}^{(2)}$ in Eq. (2) has been used in $\mathcal{L}_4^V$ and $\mathcal{L}_2^{RR}$ to eliminate superfluous operators.

Hence our theory is given by the Lagrangian:

$$\mathcal{L}_{R\chi T} = \mathcal{L}_{\chi PT}^{(2)} + \mathcal{L}_{WZW} + \mathcal{L}_{kin}^R + \mathcal{L}_2^A + \mathcal{L}_2^V + \mathcal{L}_4^V + \mathcal{L}_2^{RR}. \tag{19}$$

It is important to point out that the resonance theory constructed above is not a theory of QCD for arbitrary values of the couplings in the interaction terms. As we will see later on, these constants can be constrained by imposing well-accepted dynamical properties of the underlying theory.

III. MATRIX ELEMENT DECOMPOSITION, KINEMATICS, AND DECAY RATE

The process we are going to compute is $\tau^-(p_\tau) \to \nu_\tau(q)P^-(p)\gamma(k)$. The kinematics of this decay is equivalent to that of the radiative pion decay [51]. We will use $t := (p_\tau - q)^2 = (k + p)^2$. In complete analogy to the case of the radiative pion decay [52], the matrix element for the decay of $\tau^- \to P^-\gamma\nu_\tau$ can be written as the sum of four contributions:

$$\mathcal{M}[\tau^-(p_\tau) \to \nu_\tau(q)P^-(p)\gamma(k)]$$
$$= \mathcal{M}_{IB_\tau} + \mathcal{M}_{IB_P} + \mathcal{M}_V + \mathcal{M}_A, \tag{20}$$
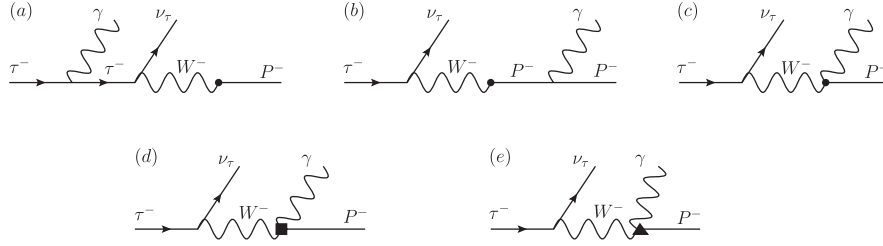
FIG. 1. Feynman diagrams for the different kinds of contributions to the radiative decays of the tau including one meson, as explained in the main text. The dot indicates the hadronization of the QCD currents. The solid square represents the SD contribution mediated by the vector current, and the solid triangle represents the SD contribution via the axial-vector current.

with[2]

$$i\mathcal{M}_{IB_\tau} = G_F V_{CKM}^{ij} e F_P p_\mu \epsilon_\nu(k) L^{\mu\nu},$$

$$i\mathcal{M}_{IB_P} = G_F V_{CKM}^{ij} e F_P \epsilon^\nu(k)\left(\frac{2p_\nu(k+p)_\mu}{m_P^2 - t} + g_{\mu\nu}\right)L^\mu,$$

$$i\mathcal{M}_V = iG_F V_{CKM}^{ij} e F_V(t)\varepsilon_{\mu\nu\rho\sigma}\epsilon^\nu(k)k^\rho p^\sigma L^\mu,$$

$$i\mathcal{M}_A = G_F V_{CKM}^{ij} e F_A(t)\epsilon^\nu(k)[(t - m_P^2)g_{\mu\nu} - 2p_\nu k_\mu]L^\mu,$$

$$\tag{21}$$

where ϵ_ν is the polarization vector of the photon. $F_V(t)$ and $F_A(t)$ are the so-called structure-dependent form factors. Finally L^μ and $L^{\mu\nu}$ are lepton currents defined by

$$L^\mu = \bar{u}_{\nu_\tau}(q)\gamma^\mu(1 - \gamma_5)u_\tau(p_\tau),$$

$$L^{\mu\nu} = \bar{u}_{\nu_\tau}(q)\gamma^\mu(1 - \gamma_5)\frac{k - \slashed{p}_\tau - M_\tau}{(k - p_\tau)^2 - M_\tau^2}\gamma^\nu u_\tau(p_\tau). \tag{22}$$

The notation introduced for the amplitudes describes the four kinds of contributions: $\mathcal{M}_{IB_\tau}$ is the internal bremsstrahlung off the tau [Fig. 1(a)]; $\mathcal{M}_{IB_P}$ is the sum of the internal bremsstrahlung off the P-meson [Fig. 1(b)] and the seagull diagram [Fig. 1(c)]; $\mathcal{M}_V$ is the SD vector contribution [Fig. 1(d)] and $\mathcal{M}_A$ is the SD axial-vector contribution [Fig. 1(e)]. Our ignorance of the exact mechanism of hadronization is parametrized in terms of the two form factors $F_A(t)$ and $F_V(t)$. In fact, these form factors are the same functions of the momentum transfer t as those in the radiative pion decay, the only difference being that t now varies from 0 up to M_τ^2 rather than just up to m_π^2.

The two matrix elements $\mathcal{M}_{IB_\tau}$ and $\mathcal{M}_{IB_P}$ are not separately gauge invariant, but their sum, i.e., the (total) matrix element for internal bremsstrahlung IB,

---

[2]Notice that i and minus factors differ with respect to Ref. [4] (Decker and Finkemeier, or DF). Moreover, our form factors have dimension of inverse mass while theirs are dimensionless. In their work, the factor of $(\sqrt{2}m_\pi)^{-1}$ in the form factors is compensated for by defining the sum over polarizations of the matrix element squared with an extra $2m_\pi^2$ factor. This should be taken into account to compare formulae in both works (using *Our* and *DF*): $F_V(t)^{DF} = \sqrt{2}m_\pi F_V(t)^{Our}$, $F_A(t)^{DF} = 2\sqrt{2}m_\pi F_A(t)^{Our}$.

$$\mathcal{M}_{IB} = \mathcal{M}_{IB_\tau} + \mathcal{M}_{IB_P}, \tag{23}$$

is indeed gauge invariant, as are $\mathcal{M}_V$ and $\mathcal{M}_A$. We also define the (total) structure-dependent radiation SD by

$$\mathcal{M}_{SD} = \mathcal{M}_V + \mathcal{M}_A. \tag{24}$$

The spinor structure can be rearranged to give

$$i\mathcal{M}_{IB} = G_F V_{ij}^{CKM} e F_P M_\tau \bar{u}_{\nu_\tau}(q)(1 + \gamma_5)$$

$$\times \left[\frac{p_\tau \cdot \epsilon}{p_\tau \cdot k} - \frac{p \cdot \epsilon}{p \cdot k} - \frac{k\slashed{\epsilon}}{2p_\tau \cdot k}\right]u_\tau(p_\tau),$$

$$i\mathcal{M}_{SD} = G_F V_{ij}^{CKM} e\{i\varepsilon_{\mu\nu\rho\sigma}L^\mu \epsilon^\nu k^\rho p^\sigma F_V(t)$$

$$+ \bar{u}_{\nu_\tau}(q)(1 + \gamma_5)$$

$$\times [(t - m_P^2)\slashed{\epsilon} - 2(\epsilon \cdot p)\slashed{k}]u(p_\tau)F_A(t)\}. \tag{25}$$

The square of the matrix element is then given by

$$\overline{|\mathcal{M}|^2} = \overline{|\mathcal{M}_{IB}|^2} + 2\overline{\mathfrak{Re}(\mathcal{M}_{IB}\mathcal{M}_{SD}^\star)} + \overline{|\mathcal{M}_{SD}|^2}, \tag{26}$$

where the bar denotes summing over the photon polarization, the neutrino spin, and averaging over the tau spin.

We follow Ref. [4] and divide the decay rate as follows: the internal bremsstrahlung part Γ_{IB} arising from $\overline{|\mathcal{M}_{IB}|^2}$, the structure-dependent part Γ_{SD} coming from $\overline{|\mathcal{M}_{SD}|^2}$, and the interference part Γ_{INT} stemming from $2\overline{\mathfrak{Re}(\mathcal{M}_{IB}\mathcal{M}_{SD}^\star)}$. Furthermore Γ_{SD} is subdivided into the vector-vector (Γ_{VV}), the axial-vector-axial-vector (Γ_{AA}), and the vector-axial-vector interference term (Γ_{VA}). Similarly, Γ_{INT} gets split into the internal bremsstrahlung-vector interference (Γ_{IB-V}) and the internal bremsstrahlung-axial-vector interference (Γ_{IB-A}) parts. Thus, one has

$$\Gamma_{ALL} = \Gamma_{IB} + \Gamma_{SD} + \Gamma_{INT},$$

$$\Gamma_{SD} = \Gamma_{VV} + \Gamma_{VA} + \Gamma_{AA}, \tag{27}$$

$$\Gamma_{INT} = \Gamma_{IB-V} + \Gamma_{IB-A}.$$

It is convenient to use the dimensionless variables x and y to proceed, as used in Ref. [4] and references therein:

$$x := \frac{2p_\tau \cdot k}{M_\tau^2}, \qquad y := \frac{2p_\tau \cdot p}{M_\tau^2}. \tag{28}$$

In the tau rest frame, x and y are the energies E_γ and E_π of the photon and the pion, respectively, expressed in units of $M_\tau/2$:

$$E_\gamma = \frac{M_\tau}{2}x, \qquad E_\pi = \frac{M_\tau}{2}y. \qquad (29)$$

Equation (29) sets the scale for the photons to be considered as "hard" or "soft." This means that the formulae for internal bremsstrahlung should be similar for radiative tau and pion decay, once they are expressed in terms of x and y, as is the case, albeit photons of comparable softness will have very different energies in both cases.

The kinematical boundaries for x and y are given by

$$0 \leq x \leq 1 - r_P^2, \qquad 1 - x + \frac{r_P^2}{1-x} \leq y \leq 1 + r_P^2, \qquad (30)$$

where

$$r_P^2 := \left(\frac{m_P}{M_\tau}\right)^2 \sim \substack{0.006 \\ 0.077} \ll 1, \qquad (31)$$

where the upper figure corresponds to $P = \pi$ and the lower one to $P = K$. It is also useful to note that

$$p \cdot k = \frac{M_\tau^2}{2}(x + y - 1 - r_P^2),$$
$$t := (p_\tau - q)^2 = (k + p)^2 = M_\tau^2(x + y - 1). \qquad (32)$$

The differential decay rate is given by Ref. [53]:

$$d\Gamma(\tau^- \to \nu_\tau P^- \gamma)$$
$$= \frac{1}{512\pi^5 E_\tau}\delta^{(4)}(k + p + q - p_\tau)\overline{|\mathcal{M}|^2}\frac{d^3\vec{k}d^3\vec{p}d^3\vec{q}}{E_\gamma E_\pi E_\nu}, \qquad (33)$$

where the bar over the matrix element denotes summing over the photon polarization, the neutrino spin and averaging over the tau spin. Choice of the tau rest frame, integration over the neutrino momentum, $\vec{p}$, and the remaining angles and introduction of x and y yield

$$\frac{d^2\Gamma}{dxdy} = \frac{m_\tau}{256\pi^3}\overline{|\mathcal{M}|^2}. \qquad (34)$$

The integration over y yields the photon spectrum

$$\frac{d\Gamma}{dx} = \int_{1-x+(r_P^2/(1-x))}^{1+r_P^2} dy \frac{d^2\Gamma}{dxdy}. \qquad (35)$$

A low-energy cut must be introduced for the photon energy because of the infrared divergence of the internal bremsstrahlung. By requiring $x \geq x_0$, one obtains the integrated decay rate

$$\Gamma(x_0) = \Gamma(E_0) = \int_{x_0}^{1-r_P^2} dx \frac{d\Gamma}{dx}, \qquad (36)$$

that does depend on the photon energy cutoff ($E_0 = \frac{M_\tau}{2}x_0$). Instead of x and y, one can also use x and z, where z is the scaled momentum transfer squared:

$$z = \frac{t}{M_\tau^2} = x + y - 1, \qquad (37)$$

whose kinematical boundaries are

$$z - r_P^2 \leq x \leq 1 - \frac{r_P^2}{z}, \qquad r_P^2 \leq z \leq 1. \qquad (38)$$

Integration of $\frac{d^2\Gamma}{dxdy}$ over x yields the spectrum in z, i.e. the spectrum in the invariant mass of the meson-photon system:

$$\frac{d\Gamma}{dz}(z) = \frac{d\Gamma}{dz}(\sqrt{t}) = \int_{z-r_P^2}^{1-r_P^2/z} dx \frac{d^2\Gamma}{dxdy}(x, y = z - x + 1). \qquad (39)$$

The integrated rate for events with $t \geq t_0$ is then given by

$$\Gamma(z_0) = \Gamma(\sqrt{t_0}) = \int_{z_0}^{1} dz \frac{d\Gamma}{dz}(z). \qquad (40)$$

We note that z_0 is both an infrared and a collinear cutoff.

In terms of the quantities defined in Eq. (27), the differential decay rate is

$$\frac{d^2\Gamma_{IB}}{dxdy} = \frac{\alpha}{2\pi}f_{IB}(x, y, r_P^2)\frac{\Gamma_{\tau^- \to \nu_\tau P^-}}{(1 - r_P^2)^2},$$

$$\frac{d^2\Gamma_{SD}}{dxdy} = \frac{\alpha}{8\pi}\frac{M_\tau^4}{F_P^2}[|F_V(t)|^2 f_{VV}(x, y, r_P^2) + 4\Re e(F_V(t)F_A^\star(t))f_{VA}(x, y, r_P^2) + 4|F_A(t)|^2 f_{AA}(x, y, r_P^2)]\frac{\Gamma_{\tau^- \to \nu_\tau P^-}}{(1 - r_P^2)^2}, \qquad (41)$$

$$\frac{d^2\Gamma_{INT}}{dxdy} = \frac{\alpha}{2\pi}\frac{M_\tau^2}{F_P}[f_{IB-V}(x, y, r_P^2)\Re e(F_V(t)) + 2f_{IB-A}(x, y, r_P^2)\Re e(F_A(t))]\frac{\Gamma_{\tau^- \to \nu_\tau P^-}}{(1 - r_P^2)^2},$$

with $\alpha = e^2/(4\pi)$ standing for the fine structure constant and

$$f_{IB}(x, y, r_P^2) = \frac{[r_P^4(x + 2) - 2r_P^2(x + y) + (x + y - 1)(2 - 3x + x^2 + xy)](r_P^2 - y + 1)}{(r_P^2 - x - y + 1)^2 x^2},$$

$$f_{VV}(x, y, r_P^2) = -[r_P^4(x + y) + 2r_P^2(1 - y)(x + y) + (x + y - 1)(-x + x^2 - y + y^2)],$$

$$f_{AA}(x, y, r_P^2) = f_{VV}(x, y, r_P^2),$$

$$f_{VA}(x, y, r_P^2) = -[r_P^2(x + y) + (1 - x - y)(y - x)](r_P^2 - x - y + 1),$$

$$f_{IB-V}(x, y, r_P^2) = -\frac{(r_P^2 - x - y + 1)(r_P^2 - y + 1)}{x},$$

$$f_{IB-A}(x, y, r_P^2) = -\frac{[r_P^4 - 2r_P^2(x + y) + (1 - x + y)(x + y - 1)](r_P^2 - y + 1)}{(r_P^2 - x - y + 1)x}. \tag{42}$$

The radiative decay rate has been expressed in terms of the width of the nonradiative decay ($\tau^- \to \nu_\tau P^-$):

$$\Gamma_{\tau^- \to \nu_\tau P^-} = \frac{G_F^2 |V_{CKM}^{ij}|^2 F_P^2}{8\pi} M_\tau^3 (1 - r_P^2)^2. \tag{43}$$

We finish this section by presenting the analytical expressions for the invariant mass spectrum:

$$\frac{d\Gamma_{IB}}{dz} = \frac{\alpha}{2\pi}[r_P^4(1 - z) + 2r_P^2(z - z^2) - 4z + 5z^2 - z^3 + (r_P^4 z + 2r_P^2 z - 2z - 2z^2 + z^3)\ln z]\frac{1}{z^2 - r_P^2 z}\frac{\Gamma_{\tau^- \to \nu_\tau P^-}}{(1 - r_P^2)^2},$$

$$\frac{d\Gamma_{VV}}{dz} = \frac{\alpha}{24\pi}\frac{M_\tau^4}{F_P^2}\frac{(z - 1)^2(z - r_P^2)^3(1 + 2z)}{z^2}|F_V(t)|^2\frac{\Gamma_{\tau^- \to \nu_\tau P^-}}{(1 - r_P^2)^2},$$

$$\frac{d\Gamma_{VA}}{dz} = 0,$$

$$\frac{d\Gamma_{AA}}{dz} = \frac{\alpha}{6\pi}\frac{M_\tau^4}{F_P^2}\frac{(z - 1)^2(z - r_P^2)^3(1 + 2z)}{z^2}|F_A(t)|^2\frac{\Gamma_{\tau^- \to \nu_\tau P^-}}{(1 - r_P^2)^2},$$

$$\frac{d\Gamma_{IB-V}}{dz} = \frac{\alpha}{2\pi}\frac{M_\tau^2}{F_P}\frac{(z - r_P^2)^2(1 - z + z\ln z)}{z}\Re e(F_V(t))\frac{\Gamma_{\tau^- \to \nu_\tau P^-}}{(1 - r_P^2)^2},$$

$$\frac{d\Gamma_{IB-A}}{dz} = -\frac{\alpha}{\pi}\frac{M_\tau^2}{F_P}[r_P^2(1 - z) - 1 - z + 2z^2 + (r_P^2 z - 2z - z^2)\ln z]\frac{z - r_P^2}{z}\Re e(F_A(t))\frac{\Gamma_{\tau^- \to \nu_\tau P^-}}{(1 - r_P^2)^2}. \tag{44}$$

The interference terms $IB - V$ and $IB - A$ are now finite in the limit $z \to r_P^2$, which proves that their infrared divergences are integrable.

Although the above formulae have been noted in Ref. [4], we independently calculate them[3] and explicitly give them here for completeness. Moreover we would like to point out that because our definitions of the form factors $F_V(t)$ and $F_A(t)$ differ from the ones given in Ref. [4], as we have mentioned before, there are some subtle differences in the above formulae between ours and theirs.

IV. STRUCTURE-DEPENDENT FORM FACTORS IN $\tau^- \to \pi^- \gamma \nu_\tau$

The Feynman diagrams, which are relevant to the vector current contributions to the SD part of the $\tau^- \to \pi^- \gamma \nu_\tau$ process, are given in Fig. 2. The analytical result is found to be

$$i\mathcal{M}_{SD_V} = iG_F V_{ud} e \bar{u}_{\nu_\tau}(q)\gamma^\mu(1 - \gamma_5)u_\tau(s)\varepsilon_{\mu\nu\alpha\beta}\epsilon^\nu(k)k^\alpha p^\beta F_V^\pi(t), \tag{45}$$

where the vector form factor $F_V^\pi(t)$ is

---

[3]We disagree with Ref. [4] on the signs of f_{VA} and f_{IB-V} in Eq. (42) and $\frac{d\Gamma_{IB-V}}{dz}$ in Eq. (44), even after taking into account the minus sign difference in the definition of the IB part.

FIG. 2.　Vector current contributions to $\tau^- \to \pi^- \gamma \nu_\tau$.

$$F_V^\pi(t) = -\frac{N_C}{24\pi^2 F_\pi} + \frac{2\sqrt{2}F_V}{3F_\pi M_V}[(c_2 - c_1 - c_5)t + (c_5 - c_1 - c_2 - 8c_3)m_\pi^2]\left[\frac{\cos^2\theta}{M_\phi^2}(1 - \sqrt{2}\text{tg}\theta) + \frac{\sin^2\theta}{M_\omega^2}(1 + \sqrt{2}\text{cotg}\theta)\right]$$

$$+ \frac{2\sqrt{2}F_V}{3F_\pi M_V}D_\rho(t)[(c_1 - c_2 - c_5 + 2c_6)t + (c_5 - c_1 - c_2 - 8c_3)m_\pi^2]$$

$$+ \frac{4F_V^2}{3F_\pi}D_\rho(t)[d_3 t + (d_1 + 8d_2 - d_3)m_\pi^2]\left[\frac{\cos^2\theta}{M_\phi^2}(1 - \sqrt{2}\text{tg}\theta) + \frac{\sin^2\theta}{M_\omega^2}(1 + \sqrt{2}\text{cotg}\theta)\right]. \qquad (46)$$

Here we have defined $D_R(t)$ as

$$D_R(t) = \frac{1}{M_R^2 - t - iM_R\Gamma_R(t)}. \qquad (47)$$

$\Gamma_R(t)$ stands for the decay width of the resonance R, which will be included following Refs. [12,39]. For completeness, we write the explicit expressions of the off-shell widths in Appendix A.

We will assume the ideal mixing case for the vector resonances ω and ϕ in any numerical application:

$$\omega_1 = \cos\theta\omega - \sin\theta\phi \sim \sqrt{\frac{2}{3}}\omega - \sqrt{\frac{1}{3}}\phi,$$

$$\omega_8 = \sin\theta\omega + \cos\theta\phi \sim \sqrt{\frac{2}{3}}\phi + \sqrt{\frac{1}{3}}\omega. \qquad (48)$$

The Feynman diagrams related to the axial-vector current contribution to the SD part are shown in Fig. 3. The corresponding result is

$$i\mathcal{M}_{SD_A} = G_F V_{ud} e\bar{u}_{\nu_\tau}(q)\gamma^\mu(1 - \gamma_5)u_\tau(s)\epsilon^\nu(k)$$
$$\times [(t - m_\pi^2)g_{\mu\nu} - 2k_\mu p_\nu]F_A^\pi(t), \qquad (49)$$

where the axial-vector form-factor $F_A^\pi(t)$ is

$$F_A^\pi(t) = \frac{F_V^2}{2F_\pi M_\rho^2}\left(1 - \frac{2G_V}{F_V}\right) - \frac{F_A^2}{2F_\pi}D_{a_1}(t)$$

$$+ \frac{\sqrt{2}F_A F_V}{F_\pi M_\rho^2}D_{a_1}(t)(-\lambda''t + \lambda_0 m_\pi^2), \qquad (50)$$

where we have used the notation

$$\sqrt{2}\lambda_0 = -4\lambda_1 - \lambda_2 - \frac{\lambda_4}{2} - \lambda_5,$$

$$\sqrt{2}\lambda'' = \lambda_2 - \frac{\lambda_4}{2} - \lambda_5 \qquad (51)$$

for the relevant combinations of the couplings in $\mathcal{L}_2^{VAP}$, Eq. (17).

V. STRUCTURE-DEPENDENT FORM FACTORS IN $\tau^- \to K^- \gamma \nu_\tau$

Although one can read the following observation from Eq. (21), let us emphasize that the model-independent part $\mathcal{M}_{IB_{\tau+K}}$ is the same as in the pion case by replacing the pion decay constant F_π with the kaon decay constant F_K. A brief explanation about this replacement is in order. The difference of F_π and F_K is generated by the low-energy constants and the chiral loops in χPT [15], while in the large N_C limit of $R\chi T$ this difference is due to the scalar resonances in an implicit way. Because of the scalar tadpole, one can always attach a scalar resonance to any of the pseudo-Goldstone boson fields, which will cause its wave function renormalization. A convenient way to count this effect is to make the scalar field redefinition before the explicit computation to eliminate the scalar tadpole effects. In the latter method, one can easily get the difference of F_π and F_K. For details, see Ref. [54] and references therein. For the model-dependent parts, the simple replacements are not applicable, and one needs to work out the corresponding form factors explicitly.

The vector current contributions to the SD part of the $\tau^- \to K^- \gamma \nu_\tau$ process are given in Fig. 4. The analytical result is found to be

FIG. 3.　Axial-vector current contributions to $\tau^- \to \pi^- \gamma \nu_\tau$.
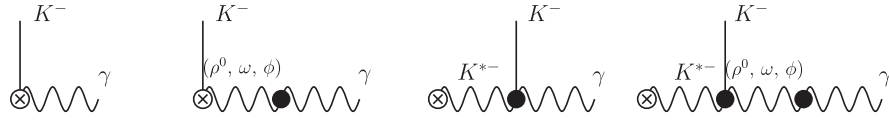
FIG. 4.   Vector current contributions to $\tau^- \to K^- \gamma \nu_\tau$.

$$i\mathcal{M}_{SD_V} = iG_F V_{us} e \bar{u}_{\nu_\tau}(q) \gamma^\mu (1 - \gamma_5) u_\tau(s) \varepsilon_{\mu\nu\alpha\beta} \epsilon^\nu(k) k^\alpha p^\beta F_V^K(t), \tag{52}$$

where the vector form factor $F_V^K(t)$ is

$$\begin{aligned}
F_V^K(t) = & -\frac{N_C}{24\pi^2 F_K} + \frac{\sqrt{2}F_V}{F_K M_V}[(c_2 - c_1 - c_5)t + (c_5 - c_1 - c_2 - 8c_3)m_K^2] \\
& \times \left[\frac{1}{M_\rho^2} - \frac{\sin^2\theta}{3M_\omega^2}(1 - 2\sqrt{2}\cot g\theta) - \frac{\cos^2\theta}{3M_\phi^2}(1 + 2\sqrt{2}\mathrm{tg}\theta)\right] \\
& + \frac{2\sqrt{2}F_V}{3F_K M_V} D_{K^*}(t)[(c_1 - c_2 - c_5 + 2c_6)t + (c_5 - c_1 - c_2 - 8c_3)m_K^2 + 24c_4(m_K^2 - m_\pi^2)] \\
& + \frac{2F_V^2}{F_K} D_{K^*}(t)[d_3 t + (d_1 + 8d_2 - d_3)m_K^2]\left[\frac{1}{M_\rho^2} - \frac{\sin^2\theta}{3M_\omega^2}(1 - 2\sqrt{2}\cot g\theta) - \frac{\cos^2\theta}{3M_\phi^2}(1 + 2\sqrt{2}\mathrm{tg}\theta)\right]. \tag{53}
\end{aligned}$$

The axial-vector current contributions to the *SD* part are given in Fig. 5. The corresponding analytical result is

$$\begin{aligned}
i\mathcal{M}_{SD_A} = & \, G_F V_{us} e \bar{u}_{\nu_\tau}(q) \gamma^\mu (1 - \gamma_5) u_\tau(s) \epsilon^\nu(k) \\
& \times [(t - m_K^2)g_{\mu\nu} - 2k_\mu p_\nu]F_A^K(t), \tag{54}
\end{aligned}$$

where the axial-vector form factor $F_A^K(t)$ is

$$\begin{aligned}
F_A^K(t) = & \frac{F_V^2}{4F_K}\left(1 - \frac{2G_V}{F_V}\right)\left(\frac{1}{M_\rho^2} + \frac{\cos^2\theta}{M_\phi^2} + \frac{\sin^2\theta}{M_\omega^2}\right) \\
& - \frac{F_A^2}{2F_K}[\cos^2\theta_A D_{K_{1H}}(t) + \sin^2\theta_A D_{K_{1L}}(t)] \\
& + \frac{F_A F_V}{\sqrt{2}F_K}[\cos^2\theta_A D_{K_{1H}}(t) + \sin^2\theta_A D_{K_{1L}}(t)] \\
& \times \left(\frac{1}{M_\rho^2} + \frac{\cos^2\theta}{M_\phi^2} + \frac{\sin^2\theta}{M_\omega^2}\right)(-\lambda''t + \lambda_0 m_K^2). \tag{55}
\end{aligned}$$

We have used the notations of K_{1H} and K_{1L} for the physical states $K_1(1400)$ and $K_1(1270)$, respectively, and the mixing angle θ_A is defined in Eq. (56) as we explain in the following.

The K_{1A} state is related to the physical states $K_1(1270)$, $K_1(1400)$ through

$$K_{1A} = \cos\theta_A K_1(1400) + \sin\theta_A K_1(1270). \tag{56}$$

The nature of $K_1(1270)$ and $K_1(1400)$ is not clear yet. It has been proposed in Ref. [55] that they result from the mixing of the states K_{1A} and K_{1B}, where K_{1A} denotes the strange partner of the axial-vector resonance a_1 with $J^{PC} = 1^{++}$, and K_{1B} is the corresponding strange partner of the axial-vector resonance b_1 with $J^{PC} = 1^{+-}$. However, in this work, we will not include the nonet of axial-vector resonances with $J^{PC} = 1^{+-}$ [56]. As argued in Ref. [55], the contributions from these resonances to tau decays are proportional to $SU(3)$-symmetry-breaking effects. Moreover, as one can see later, we will always assume $SU(3)$ symmetry for both vector and axial-vector resonances in deriving the T-matrix. For the pseudo-Goldstone bosons, physical masses will arise through the chiral symmetry-breaking mechanism in the same way as it happens in QCD. For the vector resonances, the experimental values will be taken into account in the kinematics, while in the case of the axial-vector mesons, we will take the determination of the a_1 mass from Ref. [12] and the masses of the K_1 resonances from PDG [38].

VI. CONSTRAINTS FROM QCD ASYMPTOTIC BEHAVIOR

In this part, we will exploit the asymptotic results of the form factors from perturbative QCD to constrain the resonance couplings. When discussing the high-energy constraints, we will work both in chiral and $SU(3)$ limits,

FIG. 5.   Axial-vector current contributions to $\tau^- \to K^- \gamma \nu_\tau$.

which indicates we will not distinguish the form factors with pion and kaon, which are identical in this case.[4]

For the vector form factor, the asymptotic result of perturbative QCD has been derived in Refs. [18,57]:

$$F_V^P(t \to -\infty) = \frac{F}{t}, \tag{57}$$

where F is the pion decay constant in the chiral limit. From the above asymptotic behavior, we find three constraints on the resonance couplings:

$$c_1 - c_2 + c_5 = 0, \tag{58}$$

$$c_2 - c_1 + c_5 - 2c_6 = \frac{\sqrt{2}N_C M_V}{32\pi^2 F_V} + \frac{\sqrt{2}F_V}{M_V} d_3, \tag{59}$$

$$c_2 - c_1 + c_5 - 2c_6 = \frac{3\sqrt{2}F^2}{4F_V M_V} + \frac{\sqrt{2}F_V}{M_V} d_3, \tag{60}$$

where the constraints in Eqs. (58)–(60) are derived from $\mathcal{O}(t^1)$, $\mathcal{O}(t^0)$, and $\mathcal{O}(t^{-1})$, respectively. Combining the above three constraints, we have

$$c_5 - c_6 = \frac{N_C M_V}{32\sqrt{2}\pi^2 F_V} + \frac{F_V}{\sqrt{2}M_V} d_3, \tag{61}$$

$$F = \frac{M_V \sqrt{N_C}}{2\sqrt{6}\pi}, \tag{62}$$

where the constraint of Eq. (62) has already been noticed in Refs. [4,18,57].

It is worth pointing out that different results for the asymptotic behavior of the vector form factor $F_{\pi\gamma}(t)$ have also been noted in different frameworks, such as the ones given in Refs. [58,59]. In Refs. [18,57], the result was obtained in the parton picture, and unavoidably the parton distribution function for the pion has to be imposed to give the final predictions. The OPE technique was exploited to obtain its prediction in [58], which led to the conclusion that potentially large QCD corrections could exist. In [59], the form factor was discussed by using the Bjorken-Johnson-Low theorem [60]. Variant methods have also been used to analyze this form factor: The corrections from the transverse momentum of the parton were addressed in Ref. [61]; a QCD sum rule method was applied to derive the asymptotic behavior in Ref. [62]. In the present discussion, we focus our attention on Refs. [58,59], while the study for the other results can be done analogously. Although different results agree with the same leading power of the square momentum for large t, behaving as $1/t$, they predict different coefficients. Reference [58] predicts:

$$F_V^P(t \to -\infty) = \frac{2F}{3t}, \tag{63}$$

and Ref. [59] predicts:

$$F_V^P(t \to -\infty) = \frac{F}{3t}. \tag{64}$$

By doing the same analyses as we have done by using the Lepage-Brodsky result in Eq. (57) to constrain the resonance couplings, we can straightforwardly get the constraints from the short-distance behaviors given in Eqs. (63) and (64). Apparently the matching results given in Eqs. (58) and (59) will stay the same, since they are derived from $\mathcal{O}(t^1)$ and $\mathcal{O}(t^0)$. Comparing with the result of Eq. (60) from the matching of $\mathcal{O}(t^{-1})$ by using the coefficient in Eq. (57), the corresponding results by using Eqs. (63) and (64) are, for Ref. [58],

$$c_2 - c_1 + c_5 - 2c_6 = \frac{F^2}{2\sqrt{2}F_V M_V} + \frac{\sqrt{2}F_V}{M_V} d_3, \tag{65}$$

and for Ref. [59],

$$c_2 - c_1 + c_5 - 2c_6 = \frac{F^2}{4\sqrt{2}F_V M_V} + \frac{\sqrt{2}F_V}{M_V} d_3, \tag{66}$$

which lead to the following results by combining Eqs. (58) and (59), namely, for Ref. [58],

$$F = \frac{M_V \sqrt{N_C}}{4\pi}, \tag{67}$$

and for Ref. [59],

$$F = \frac{M_V \sqrt{N_C}}{2\sqrt{2}\pi}. \tag{68}$$

The formulae displayed in Eqs. (62), (67), and (68) provide a simple way to discriminate between different asymptotic behaviors. The chiral limit values for the pion decay constant F and the mass of the lowest vector multiplet M_V have been thoughtfully studied at the leading order of $1/N_C$ in Ref. [63], which predicts $F = 90.8$ MeV and $M_V = 764.3$ MeV. The different results shown in Eqs. (62), (67), and (68) from matching different short-distance behaviors of Refs. [18,58,59] deviate from the phenomenology study at the level of 5%, 16%, and 64%, respectively,[5] which implies that the short-distance behavior in Eq. (57) is more reasonable than the ones in Eqs. (63) and (64). Hence for the matching result at the order of $1/t$, we will use the one in Eq. (62) throughout the following discussion. However we stress that the inclusion of extra multiplets of vector resonances or the subleading corrections in $1/N_C$ may alter the current conclusion.

The high-energy constraints on the resonance couplings c_i and d_i have been studied in different processes. The OPE analysis of the VVP Green function gives [34]

---

[4]The results of this procedure are independent of taking the chiral limit [34].

[5]The results are mildly changed when estimating the values of F and M_V by F_π and M_ρ respectively, as expected.

$$c_5 - c_6 = \frac{N_C M_V}{64\sqrt{2}\pi^2 F_V}, \qquad (69)$$

$$d_3 = -\frac{N_C M_V^2}{64\pi^2 F_V^2} + \frac{F^2}{8F_V^2}. \qquad (70)$$

The constraint from $\tau^- \to (VP)^- \nu_\tau$ study leads to

$$c_5 - c_6 = -\frac{F_V}{\sqrt{2}M_V}d_3, \qquad (71)$$

if one neglects the heavier vector resonance multiplet [10].

The results from the analysis of $\tau^- \to (KK\pi)^- \nu_\tau$ are [64]

$$c_5 - c_6 = \frac{N_C M_V F_V}{192\sqrt{2}\pi^2 F^2}, \qquad d_3 = -\frac{N_C M_V^2}{192\pi^2 F^2}. \quad (72)$$

It is easy to check that the results of Eqs. (71) and (72) are consistent. Combining Eqs. (61) and (71) leads to

$$c_5 - c_6 = \frac{N_C M_V}{64\sqrt{2}\pi^2 F_V}, \qquad d_3 = -\frac{N_C M_V^2}{64\pi^2 F_V^2}, \quad (73)$$

where the constraint of $c_5 - c_6$ is consistent with the result from the OPE analysis of the VVP Green function [34], while the result of d_3 is not.

By demanding the consistency of the constraints derived from the processes of $\tau^- \to P^- \gamma \nu_\tau$ and $\tau^- \to (VP)^- \nu_\tau$ given in Eq. (73) and the results from $\tau^- \to (KK\pi)^- \nu_\tau$ given in Eq. (72), we get the following constraint:

$$F_V = \sqrt{3}F. \qquad (74)$$

If one combines the high-energy constraint from the two pion vector form factor [37],

$$F_V G_V = F^2, \qquad (75)$$

and the result of Eq. (74) we get here, the modified Kawarabayashi-Suzuki-Riazuddin-Fayyazuddin relation [65,66] is derived:

$$F = \sqrt{3}G_V, \qquad (76)$$

which is also obtained in the partial wave dispersion relation analysis of $\pi\pi$ scattering by properly including the contributions from the crossed channels [67].

Although the branching ratios for the modes of $\tau \to P\gamma\nu_\tau$ which we are discussing could be higher than for some modes that have already been detected, they have not been observed yet. Lacking experimental data, we will make some theoretically and phenomenologically based assumptions in order to present our predictions for the spectra and branching ratios.

Taking into account the previous relations, one would have $F_V^\pi(t)$ in terms of $c_1 + c_2 + 8c_3 - c_5$ and $d_1 + 8d_2 - d_3$. For the first combination, $c_1 + c_2 + 8c_3 - c_5 = c_1 + 4c_3$ ($c_1 - c_2 + c_5 = 0$ has been used), the prediction for $c_1 + 4c_3$ in [34] yields $c_1 + c_2 + 8c_3 - c_5 = 0$. In Ref. [34], the other relevant combination of couplings is also restricted: $d_1 + 8d_2 - d_3 = \frac{F^2}{8F_V^2}$. In $F_V^K(t)$, c_4 appears, in addition. There is a phenomenological determination

of this coupling in the study of the $KK\pi$ decay modes of the τ [11]: $c_4 = -0.07 \pm 0.01$.

Turning now to the axial-vector form factor, it still depends on four couplings in both channels: F_A, M_A, λ'', and λ_0. If one invokes the once-subtracted dispersion relation for the axial-vector form factor, as done in Ref. [4], one cannot get any constraints on the resonance couplings from the axial-vector form factors given in Eqs. (50) and (55). In fact, by demanding the form factor to satisfy the unsubtracted dispersion relation, which guarantees a better high-energy limit, we can get the following constraint:

$$\lambda'' = \frac{2G_V - F_V}{2\sqrt{2}F_A}, \qquad (77)$$

which has been already noted in Ref. [35].

In order to constrain the free parameters as much as possible, we decide to exploit the constraints from the Weinberg sum rules [68]: $F_V^2 - F_A^2 = F^2$ and $M_V^2 F_V^2 - M_A^2 F_A^2 = 0$, yielding

$$F_A = 2F^2, \qquad M_A = \frac{6\pi F}{\sqrt{N_C}}. \qquad (78)$$

For the axial-vector resonance coupling λ_0, we use the result from Refs. [12,35]:

$$\lambda_0 = \frac{G_V}{4\sqrt{2}F_A}. \qquad (79)$$

To conclude this section, we summarize the previous discussion on the high-energy constraints:

$$F_V = \sqrt{3}F, \qquad G_V = \frac{F}{\sqrt{3}}, \qquad F_A = \sqrt{2}F,$$

$$M_V = \frac{2\sqrt{6}\pi F}{\sqrt{N_C}}, \qquad M_A = \frac{6\pi F}{\sqrt{N_C}}, \qquad \lambda_0 = \frac{1}{8\sqrt{3}}, \quad (80)$$

$$\lambda'' = -\frac{1}{4\sqrt{3}}, \qquad c_5 - c_6 = \frac{\sqrt{N_C}}{32\pi}, \qquad d_3 = -\frac{1}{8}.$$

In the above results, we have discarded the constraint in Eq. (70), which is the only result inconsistent with the others.

VII. PHENOMENOLOGICAL DISCUSSION

Apart from the parameters we mentioned in the last section, there is still one free coupling θ_A, which describes the mixing of the strange axial-vector resonances in Eq. (56). The value of θ_A has already been determined in the literature [10,55,69]. We recapitulate the main results in the following.

Reference [55] has given $\theta_A \sim 33°$. In Ref. [10], $|\theta_A| \sim 58.1°$ is determined through the considered decays $\tau^- \to (VP)^- \nu_\tau$. In Ref. [69], the study of $\tau \to K_1 \nu_\tau$ gives $|\theta_A| = {}^{37°}_{58°}$ as the two possible solutions. The decay $D \to K_1 \pi$ allows us to conclude that θ_A must be negative, and it is pointed out that the observation of $D^0 \to K_1^- \pi^+$
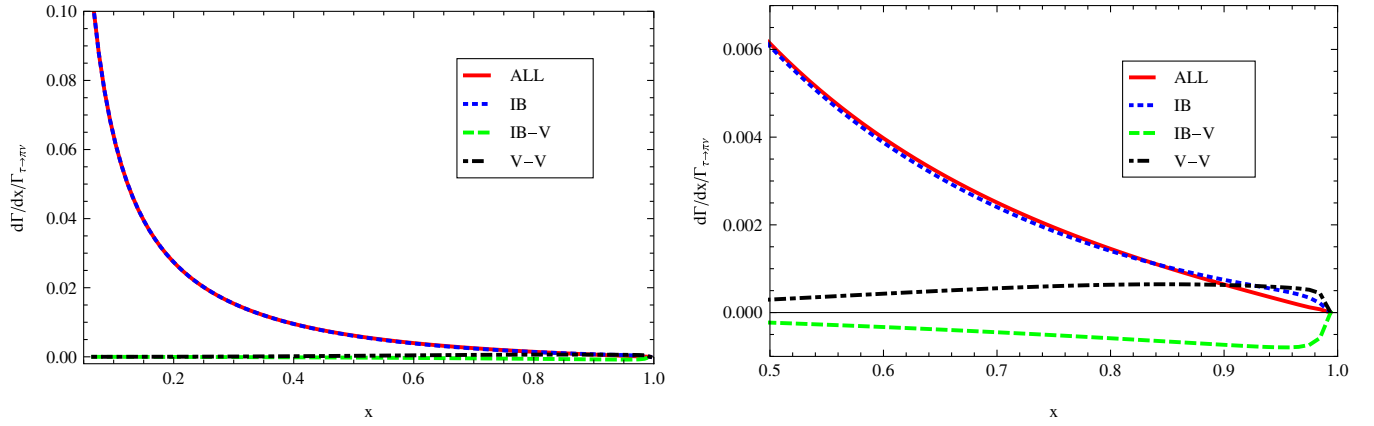
FIG. 6 (color online). Differential decay width (in units of $\Gamma_{\tau \to \pi \nu_\tau}$) of the process $\tau^- \to \pi^- \gamma \nu_\tau$, including only the model-independent contributions as a function of x. For the form factors, only the WZW term is considered for this estimate, where the axial vector contribution is absent. The right plot is the close-up of the left one in the region of $x > 0.5$.

with a branching ratio $\sim 5 \times 10^{-4}$ would imply $\theta_A \sim -58°$. However, a later analysis in Ref. [70] finds that the current measurement of $\bar{B}^0 \to K_1^-(1400)\pi^+$ [38] favors a mixing angle of $-37°$ over $-58°$. In this respect, the relation

$$|\Gamma(J/\Psi \to K_1^0(1400)\bar{K}^0)|^2$$
$$= \text{tg}\theta_A^2 |\Gamma(J/\Psi \to K_1^0(1270)\bar{K}^0)|^2 \quad (81)$$

would be very useful to get θ_A, once these modes are detected. In the following discussion, we will show the results using both $|\theta_A| = 37°$ and $58°$. The other inputs are given in Appendix B.

A. Results with only *WZW* contribution

As stated before, it is strange that the decay modes $\tau \to P\gamma\nu_\tau$ have not been detected so far. The most naïve and completely model-independent estimate would be to just include the IB part and the WZW contribution to the VV part, as the latter is completely fixed by QCD. We know that, doing it this way, we are losing the contribution of vector and axial-vector resonances, which should be important in the high-x region. However, even doing so, one is able to find that the radiative decay $\tau^- \to \pi^-\gamma\nu_\tau$ has a decay probability larger than the mode $\tau^- \to K^+ K^- K^- \nu_\tau$.[6] For a reasonably low cutoff on the photon energy, this conclusion holds for the $\tau^- \to K^-\gamma\nu_\tau$ as well.

Before seeing this, we will discuss briefly the meaning of cutting on the photon energy.[7] As is well known [71,72], the IR divergences due to the vanishing photon mass cancel when considering at the same time the nonradiative and the radiative decays with one photon.[8] In practice, this trans-

lates into mathematical language the physical notion that the detectors have a limited angular resolution that defines a threshold detection angle for photons. If one considers a photon emitted with a smaller angle, it should be counted together with the nonradiative decay, as it is effectively measured in this way. The sum is of course an IR-safe observable. The splitting depends on the particular characteristics of the experimental setting. Obviously, the branching fraction for the radiative decay depends on this cutoff energy. We will consider here the case $E_{\gamma\text{thr}} = 50$ MeV, which corresponds to $x = 0.0565$. In order to illustrate the dependence on this variable, we will also show the extremely conservative case of $E_{\gamma\text{thr}} = 400$ MeV ($x = 0.45$). In the first case, we obtain $\Gamma(\tau^- \to \pi^-\gamma\nu_\tau) = 3.182 \times 10^{-15}$ GeV, and, in the second case, we are still above the $3K$ decay width, $\Gamma(\tau^- \to \pi^-\gamma\nu_\tau) = 3.615 \times 10^{-16}$ GeV. In Fig. 6 we plot the photon spectrum of $\tau^- \to \pi^-\gamma\nu_\tau$. Proceeding analogously for the decay with a K^-, we find: $\Gamma(\tau^- \to K^-\gamma\nu_\tau) = 6.002 \times 10^{-17}$ GeV for $E_{\gamma\,\text{thr}} = 50$ MeV, and $\Gamma(\tau^- \to K^-\gamma\nu_\tau) = 4.589 \times 10^{-18}$ GeV for $E_{\gamma\,\text{thr}} = 400$ MeV. The photon spectrum of $\tau^- \to K^-\gamma\nu_\tau$ can be seen in Fig. 7. For any reasonable cut on E_γ, these modes should have already been detected by the B-factories.

Already at this level of the phenomenological analysis, the question of the accuracy of the detection of soft photons at the B-factories [73] arises.[9] An error larger than expected (here and in some undetected particle interpreted as missing energy, in addition to a Gaussian treatment of systematic errors) could enlarge the uncertainty claimed on the measurement of $B^- \to \tau^- \nu_\tau$ [38] when combining the Belle [75] and BABAR measurements [76,77], taking it closer to the standard model expectations.

---

[6] $\Gamma(\tau^- \to K^+ K^- K^- \nu_\tau) = 3.579(66) \times 10^{-17}$ GeV.
[7] A cut on the photon energy was introduced in Sec. III.
[8] In general, the IR divergences of the n-photon decay are canceled by those in the $n + 1$-photon process.
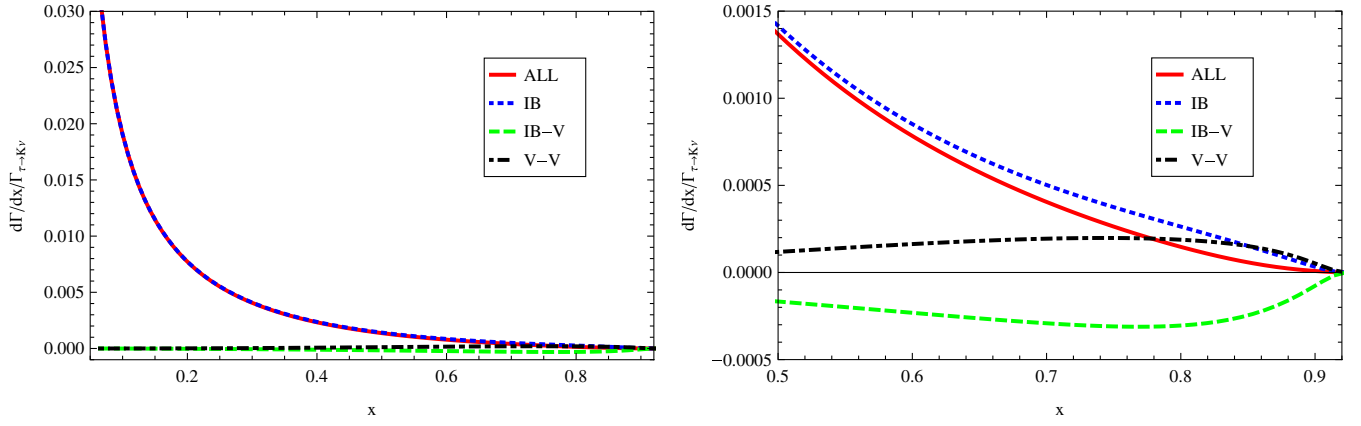
[9] See however, Ref. [74].

FIG. 7 (color online). Differential decay width (in units of $\Gamma_{\tau \to K \nu_\tau}$) of the process $\tau^- \to K^- \gamma \nu_\tau$, including only the model-independent contributions as a function of x. For the form factors, only the *WZW* term is considered for this estimate, where the axial vector contribution is absent. The right plot is the close-up of the left plot in the region of $x > 0.5$.

B. Results with the resonance contributions for the pion channel

Next we also include the model-dependent contributions. Since in the kaon channel there are uncertainties associated with the off-shell width of the strange axial-vector resonance and the mixing of the corresponding light

and heavy states, we will present first the pion channel where there are no uncertainties of these types and everything is fixed.

In Fig. 8, the resulting photon spectrum of the process $\tau^- \to \pi^- \gamma \nu_\tau$ is displayed. In order to display clearly how the different parts contribute to the spectrum, we have

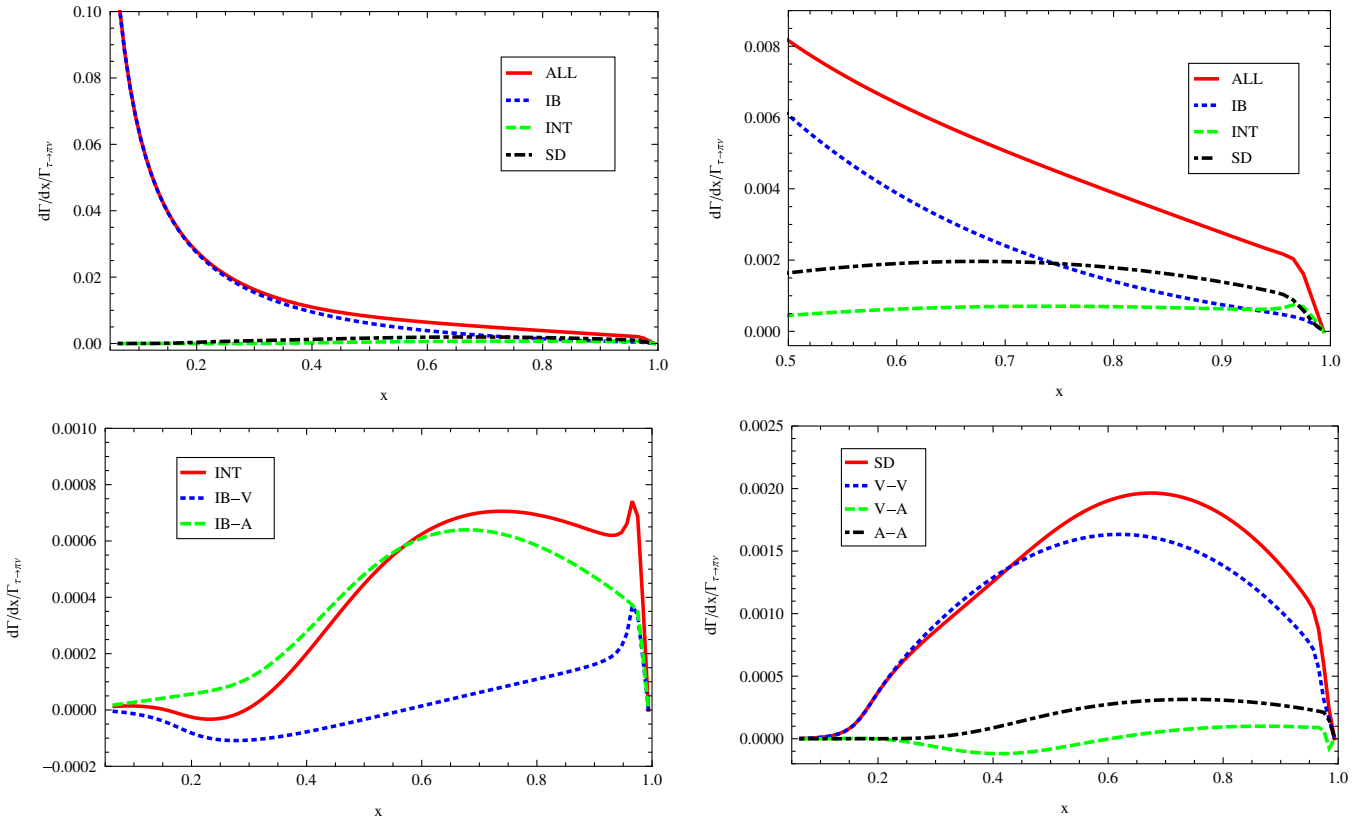FIG. 8 (color online). Differential decay width (in units of $\Gamma_{\tau \to \pi \nu_\tau}$) of the process $\tau^- \to \pi^- \gamma \nu_\tau$, including all contributions as a function of x. The top right plot is the close-up of the top left plot in the region of $x > 0.5$. The bottom left and right plots display the compositions of the interference and structure-dependent parts, respectively.

given the close-up of the spectrum for the high x region and also shown the separate contributions. For "soft" photons ($x_0 \lesssim 0.3$) the internal bremsstrahlung dominates completely. One should note that, for very soft photons, the multiphoton production rate becomes important, so that our $\mathcal{O}(\alpha)$ results are not reliable too close to the IR divergence $x = 0$. We qualitatively agree with the results in the Decker and Finkemeier (DF) papers, for the same order of α to the three significant figures shown in Ref. [4].

The spectrum is significantly enhanced by SD contributions for hard photons ($x_0 \gtrsim 0.4$), as we can see in Fig. 8. From Fig. 8 one can also see that the vector current contribution mediated by the vector resonances dominates the SD part. The interference terms between the bremsstrahlung and the SD parts are also shown in Fig. 8. If we compare the predicted curves with those in Ref. [4], we see that the qualitative behavior is similar: the IB contribution dominates up to $x \sim 0.75$. For larger photon energies, the SD part is predominant due to the VV contribution and overcomes the SI part. We confirm the peak and shoulder structure shown at $x \sim 1$ in the interference contribution, which is essentially due to the $IB - V$ term, and also the $V - A$ term, which is in any case tiny.

While the integration over the IB part needs an IR cutoff, the SD part does not. We have performed the integration over the complete phase space,[10] yielding:

$$\Gamma_{VV} = 0.99 \times 10^{-3}, \qquad \Gamma_{VA} \sim 0,$$
$$\Gamma_{AA} = 0.15 \times 10^{-3} \Rightarrow \Gamma_{SD} = 1.14 \times 10^{-3}. \qquad (82)$$

Our number for Γ_{SD} lies between the results for the monopole and the tripole parametrizations in Ref. [4]. However, they get a smaller (larger) $VV(AA)$ contribution than we do by $\sim 20\%(\sim 200\%)$. This last discrepancy is due to the off-shell a_1 width they use. In fact, if we use the constant width approximation, we get a number very close to theirs for the AA contribution. With the understanding of the a_1 width in the $\tau \to 3\pi\nu_\tau$ observables [12], we can say that their (relatively) high AA contribution is an artifact of the ad-hoc off-shell width used. Since the numerical difference in varied vector off-shell widths is not that high, the numbers for VV are closer.

The numbers in Eq. (82) are translated into the following branching ratios (BR):

$$\mathrm{BR}_{VV}(\tau \to \pi\gamma\nu_\tau) = 1.05 \times 10^{-4},$$
$$\mathrm{BR}_{AA}(\tau \to \pi\gamma\nu_\tau) = 0.15 \times 10^{-4}. \qquad (83)$$

We can also compare the VV value with the narrow-width estimate. Taking into account the lowest-lying resonance $\rho(770)$, we get

---

[10]Here and in what follows, all contributions to the partial decay width are given in units of the nonradiative decay.

$$\mathrm{BR}_{VV}(\tau \to \pi\gamma\nu_\tau) \sim \mathrm{BR}(\tau \to \rho\nu_\tau) \times \mathrm{BR}(\rho \to \pi\gamma)$$
$$\sim \mathrm{BR}(\tau \to \pi^-\pi^0\nu_\tau)\mathrm{BR}(\rho \to \pi\gamma)$$
$$\sim 25.52\% \times 4.5 \times 10^{-4} = 1.15 \times 10^{-4}, \qquad (84)$$

which is quite a good approximation.

In Table I we display (for two different values of the photon energy cutoff) how the different parts contribute to the total rate. For a low-energy cutoff, most of the rate comes from IB, while for a higher-energy cutoff, the SD parts (particularly the VV contribution) gain importance. While the VA contribution is always negligible, the $IB - V$, $IB - A$, and the remaining SD parts (VV and AA) have some relevance for a higher-energy cutoff.

In Fig. 9, we show the pion-photon invariant spectrum. We find a much better signal of the SD contributions as compared with the photon spectrum in Fig. 8, which has already been noticed in Ref. [4]. Then, the pion-photon spectrum is better suited to study the SD effects. In this case, the VA part is identically zero, since this interference vanishes in the invariant mass spectrum after integration over the other kinematic variable. Of course, in the VV spectrum, we see the shape of the ρ contribution neatly, as shown in Fig. 9, where on the contrary the a_1 exchange in AA has a softer and broader effect. The $IB - SD$ radiation near the a_1 is dominated by $IB - A$, which gives the positive contribution to the decay rate. While near the energy region of the ρ resonance, we find the $IB - SD$ contribution to be negative as driven by $IB - V$ there. In the whole spectrum, only the ρ resonance manifests as a peak, and one can barely see the signal of a_1, mainly due to its broad width.

C. Results with the resonance contributions for the kaon channel

Next we turn to the $\tau^- \to K^-\gamma\nu_\tau$ channel. In this case, several sources of uncertainty make our prediction less controlled than in the $\tau^- \to \pi^-\gamma\nu_\tau$ case. We comment on them in turn.

TABLE I. Contributions of the different parts to the total rate in the decay $\tau^- \to \pi^-\gamma\nu_\tau$ (in units of $\Gamma_{\tau \to \pi\nu}$), using two different cutoffs for the photon energy: $E_\gamma = 50$ MeV ($x_0 = 0.0565$) and $E_\gamma = 400$ MeV ($x_0 = 0.45$).

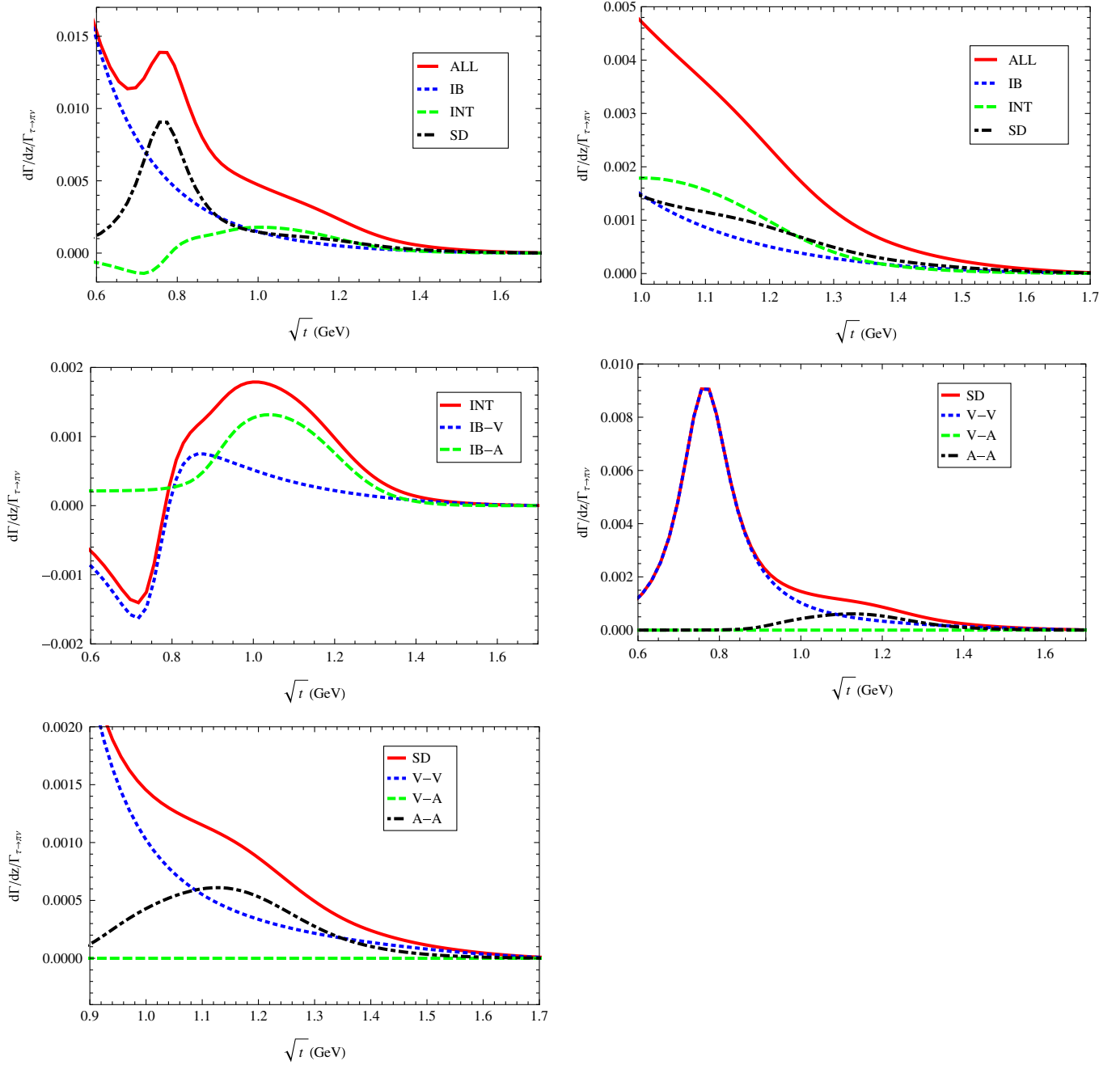|	$x_0 = 0.0565$	$x_0 = 0.45$
IB	13.09×10^{-3}	1.48×10^{-3}
$IB - V$	0.02×10^{-3}	0.04×10^{-3}
$IB - A$	0.34×10^{-3}	0.29×10^{-3}
VV	0.99×10^{-3}	0.73×10^{-3}
VA	~ 0	0.02×10^{-3}
AA	0.15×10^{-3}	0.14×10^{-3}
ALL	14.59×10^{-3}	2.70×10^{-3}

FIG. 9 (color online). Differential decay width (in units of $\Gamma_{\tau \to \pi \nu_\tau}$) of the process $\tau^- \to \pi^- \gamma \nu_\tau$, including all contributions as a function of $\sqrt{t}$. The top right plot is the close-up of the top left plot in the region of $\sqrt{t} > 1.0$. The middle left and right plots display the compositions of the interference and structure-dependent parts, respectively. The bottom plot is the close-up of the middle right plot in the region of $\sqrt{t} > 0.9$ GeV.

Concerning the vector form-factor contribution, no uncertainty is associated with the off-shell widths of the vector resonances, which are implemented as we explained before. However, we have observed that the VV contribution to the decay rate is much larger (up to 1 order of magnitude, even for a low-energy cutoff) than the IB one for $c_4 \sim -0.07$, a feature that is unexpected. In this case, one would also see a prominent bump in the spectrum, contrary to the typical monotonous fall driven by the IB term. For smaller values of $|c_4|$, this bump reduces its magnitude and finally disappears. Also, one should not forget that the inclusion of a second multiplet of resonances may vary this conclusion.

The uncertainty in the axial-vector form factors is two-fold: On one side, there is a broad band of allowed values for θ_A, as discussed at the beginning of this section. On the other hand, since we have not performed the analyses of the decay $\tau \to K \pi \pi \nu_\tau$ modes yet, we do not have an off-shell

TABLE II. Contributions of the different parts to the total rate in the decay $\tau^- \to K^- \gamma \nu_\tau$ (in units of $\Gamma_{\tau \to K\nu}$), using two different cutoffs for the photon energy: $E_\gamma = 50$ MeV ($x_0 = 0.0565$) and $E_\gamma = 400$ MeV ($x_0 = 0.45$) and also different values of the resonance couplings. The numbers in parentheses denote the corresponding results with $|\theta_A| = 37°$, while the other numbers are obtained with $|\theta_A| = 58°$.

	$x_0 = 0.0565, c_4 = -0.07$ $\|\theta_A\| = 58°(37°)$	$x_0 = 0.0565, c_4 = 0$ $\|\theta_A\| = 58°(37°)$	$x_0 = 0.45, c_4 = -0.07$ $\|\theta_A\| = 58°(37°)$	$x_0 = 0.45, c_4 = 0$ $\|\theta_A\| = 58°(37°)$
IB	3.64×10^{-3}	3.64×10^{-3}	0.31×10^{-3}	0.31×10^{-3}
IB − V	0.69×10^{-3}	0.10×10^{-3}	0.83×10^{-3}	0.12×10^{-3}
IB − A	$0.22(0.25) \times 10^{-3}$	$0.22(0.25) \times 10^{-3}$	$0.15(0.18) \times 10^{-3}$	$0.15(0.18) \times 10^{-3}$
VV	58.55×10^{-3}	1.30×10^{-3}	29.04×10^{-3}	0.66×10^{-3}
VA	$\sim 0(\sim 0)$	$\sim 0(\sim 0)$	$0.09(0.09) \times 10^{-3}$	$0.01(0.01) \times 10^{-3}$
AA	$0.13(0.16) \times 10^{-3}$	$0.13(0.16) \times 10^{-3}$	$0.12(0.15) \times 10^{-3}$	$0.12(0.15) \times 10^{-3}$
ALL	$63.23(63.29) \times 10^{-3}$	$5.39(5.45) \times 10^{-3}$	$30.54(30.60) \times 10^{-3}$	$1.37(1.43) \times 10^{-3}$

width derived from a Lagrangian for the K_{1A} resonances. In the $\tau \to 3\pi\nu_\tau$ decays, Γ_{a_1} has the starring role [12]. Since the K_{1A} meson widths are much smaller (90 ± 20 MeV and 174 ± 13 MeV, for the $K_1(1270)$ and $K_1(1400)$, respectively) and they are hardly close to the on-shell condition, a rigorous description of the width is not an unavoidable ingredient for a reasonable estimate. We decided to use the expression inspired by the ρ width from

Ref. [39]. The explicit forms of the K_{1A} off-shell widths which we follow are given in Appendix A.

Considering all the sources of uncertainty mentioned, we will content ourselves with giving our predictions for the case of $c_4 = 0, -0.07$, and $|\theta_A| = 58°, 37°$. We first show the results of the decay rates in Table II. The lesson we can learn from the numbers in Table II is that the decay rate is sensitive to the value of c_4, while different choices of
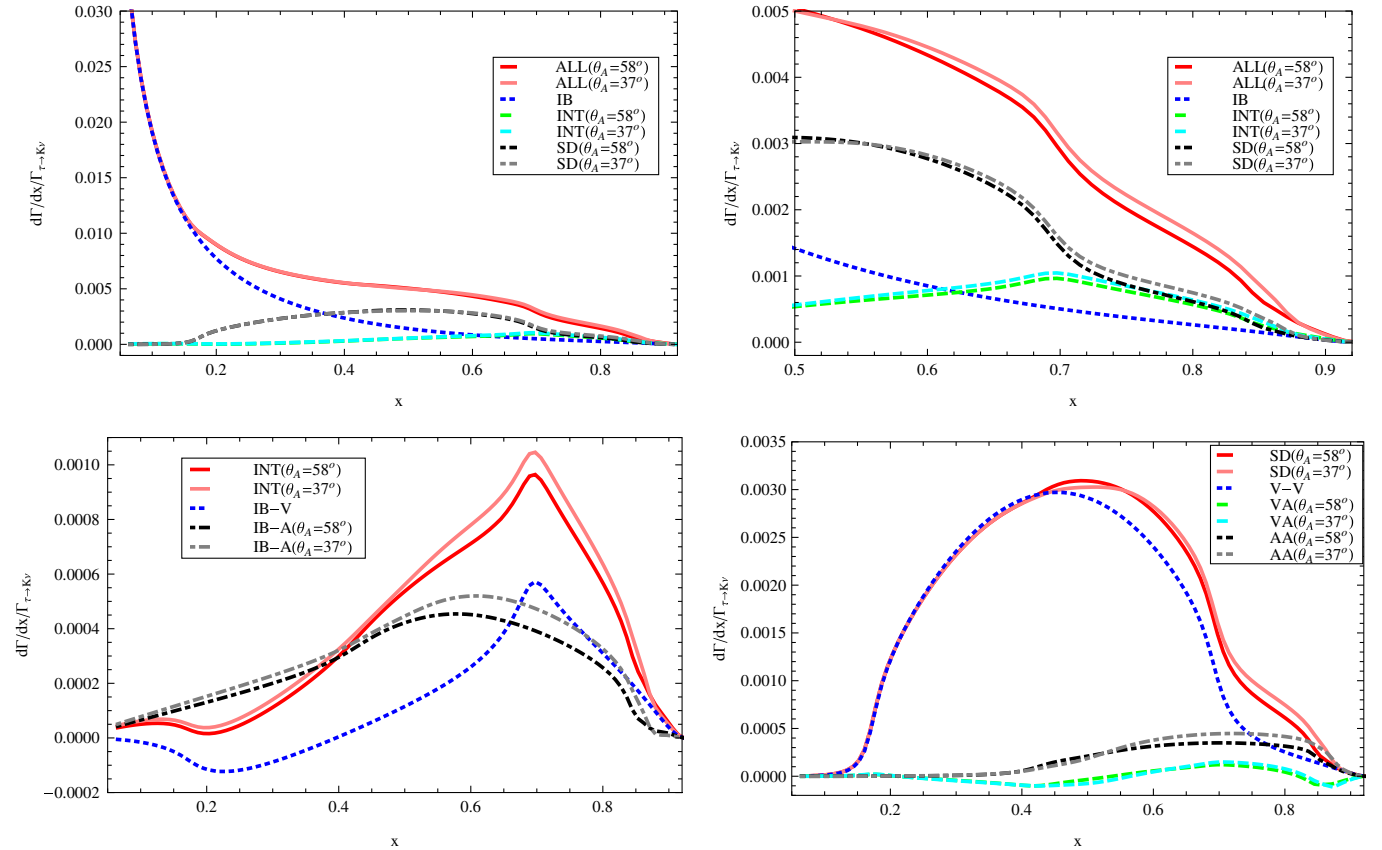

FIG. 10 (color online). Differential decay width (in units of $\Gamma_{\tau \to K\nu_\tau}$) of the process $\tau^- \to K^- \gamma \nu_\tau$, including all contributions as a function of x with $c_4 = 0$. The top right plot is the close-up of the top left plot in the region of $x > 0.5$. The bottom left and right plots display the compositions of the interference and structure-dependent parts, respectively.
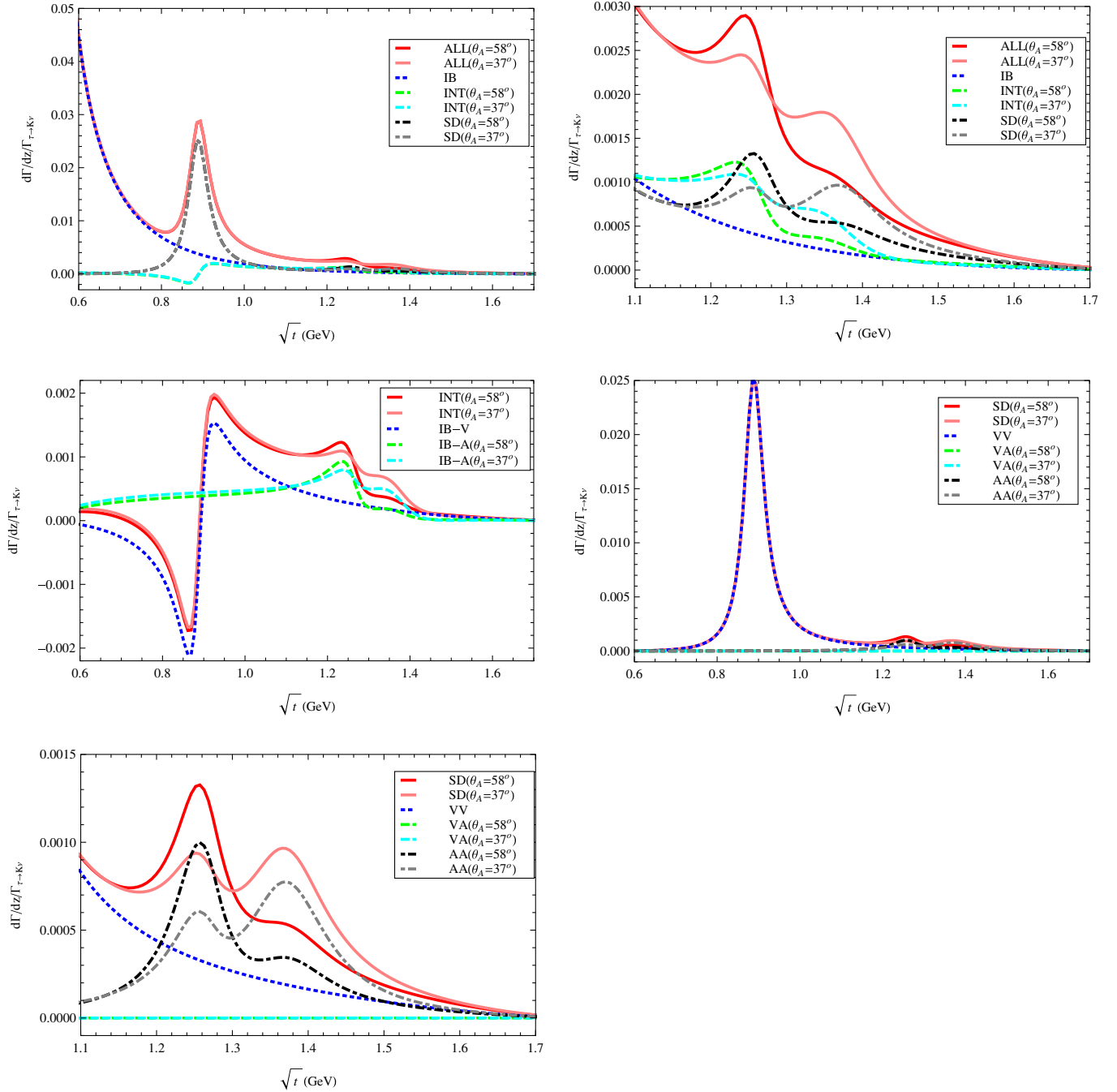
FIG. 11 (color online). Differential decay width (in units of $\Gamma_{\tau \to K\nu_\tau}$) of the process $\tau^- \to K^- \gamma \nu_\tau$, including all contributions as a function of $\sqrt{t}$ with $c_4 = 0$. The top right plot is the close-up of the top left plot in the region of $\sqrt{t} > 1.1$ GeV. The middle left and right plots display the compositions of the interference and structure-dependent parts, respectively. The bottom plot is the close-up of the middle right plot in the region of $\sqrt{t} > 1.1$ GeV.

θ_A barely influence the final results. In order to illustrate our predictions, we present in Figs. 10 and 11 the plots analogous to those we discussed in the $\tau^- \to \pi^- \gamma \nu_\tau$ channel for the case $c_4 = 0$ and $|\theta_A| = 37°$, $58°$. For $c_4 = -0.07$, we give the plots in Figs. 12 and 13, where one can see that the VV contribution from the SD parts overwhelmingly dominates almost the whole spectrum.

VIII. CONCLUSIONS

In this article we have studied the radiative one-meson decays of the τ: $\tau^- \to (\pi/K)^- \gamma \nu_\tau$. We have computed the relevant form factors for both channels and obtained the asymptotic conditions on the couplings imposed by the high-energy behavior of these form factors, dictated by QCD. The relations that we have found here are compatible
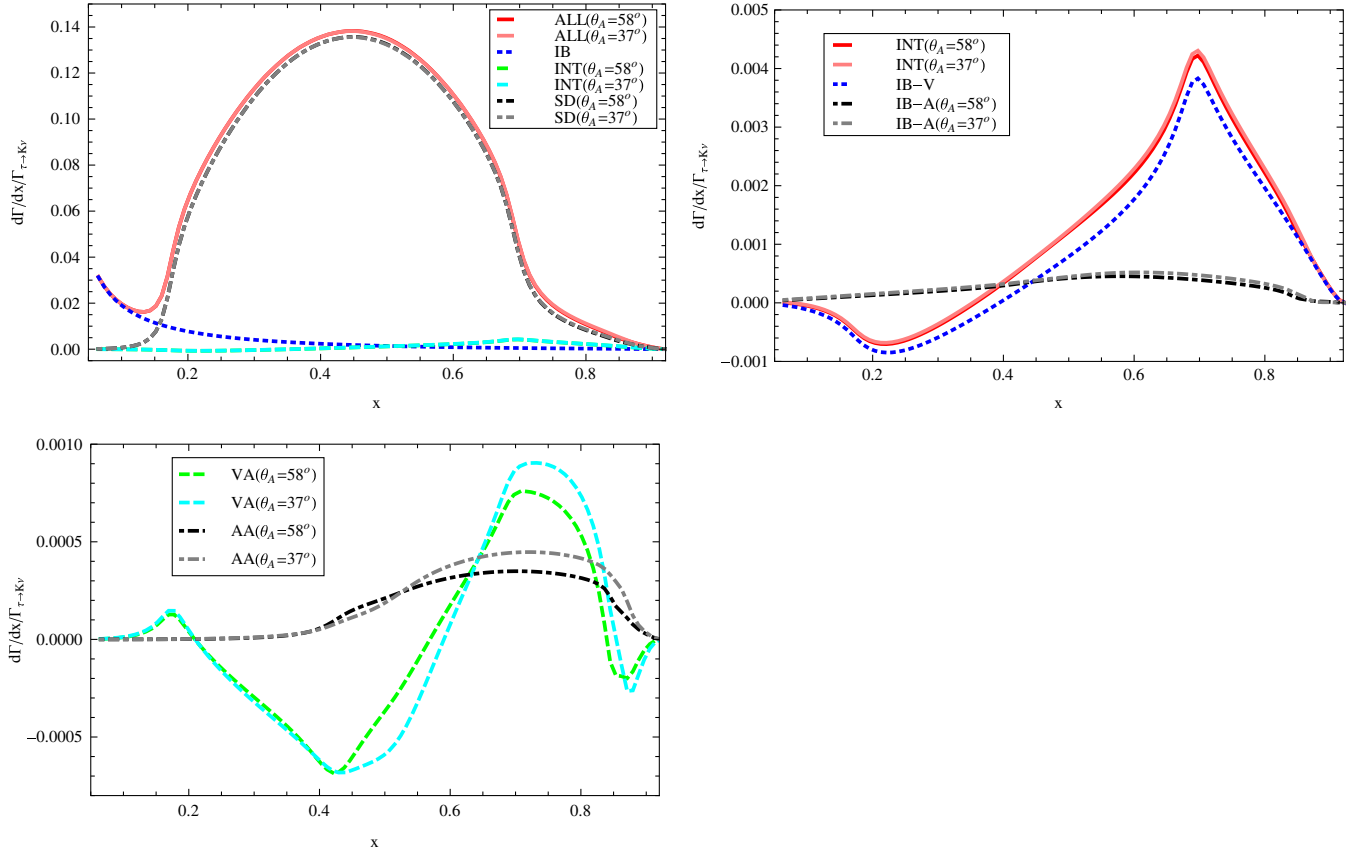
FIG. 12 (color online).   Differential decay width (in units of $\Gamma_{\tau \to K\nu_\tau}$) of the process $\tau^- \to K^- \gamma \nu_\tau$, including all contributions as a function of x with $c_4 = -0.07$. The top right plot shows the compositions of the interference parts. The bottom left one shows the VA and AA contributions.

with those found in other phenomenological applications of the theory.

One of our motivations to examine these processes is that they have not been detected yet, according to naïve estimates or to Breit-Wigner parametrizations. We have checked the existing computations for the IB part. Adding to it the WZW contribution, that is, the LO contribution in χPT coming from the QCD anomaly, we have estimated the model-independent contribution to both decays that could be taken as a lower bound. The values that we obtain for the π channel are at least 1 order of magnitude above the already-observed $3K$ decay channel even for a high-energy cutoff on the photon energy. In the K channel, the model-independent contribution gives a branching ratio larger than that of the $3K$ decay channel, as well. Only by imposing a large cutoff on E_γ could one understand that the latter mode has not been detected so far. We expect, then, that upcoming measurements at B- and tau-charm factories will bring the discovery of these tau decay modes in the near future.

We do not have any free parameter in the $\tau^- \to \pi^- \gamma \nu_\tau$ decay, and that allows us to make a complete study. Since the IB contribution dominates, it will require some statistics to study the SD effects. In this sense, the analysis of the

π-photon spectrum (t-spectrum) is more promising than that of the pure photon spectrum (x-spectrum), as we have shown. We are eager to see whether the discovery of this mode confirms our findings, since we believe that the uncertainties of our study are small for this channel.

As expected, the higher mass of the kaon makes easier the observation of SD effects. However, there are several sources of uncertainty in the $\tau^- \to K^- \gamma \nu_\tau$ decay that prevent us from having a definitive prediction for this channel. The most important one raises some doubts either about the value of c_4, a parameter describing the $SU(3)$-breaking effect, obtained in Ref. [11] or on the sufficiency of one multiplet of vector resonances to describe this decay. We point out that the inclusion of the heavier multiplets of resonances will not only directly give contributions to the spectra and the decay rates, but also influence the final results in an indirect way by entering the resonance parameters given in Eq. (80). As we have shown, the value of this coupling drastically affects the strength of the VV (and thus the whole SD) contribution. Besides, there is an uncertainty associated with the broad band of allowed values for θ_A. However, the AA contribution is not important anyway with respect to that on c_4. Even smaller is the error associated with the off-shell width behavior of
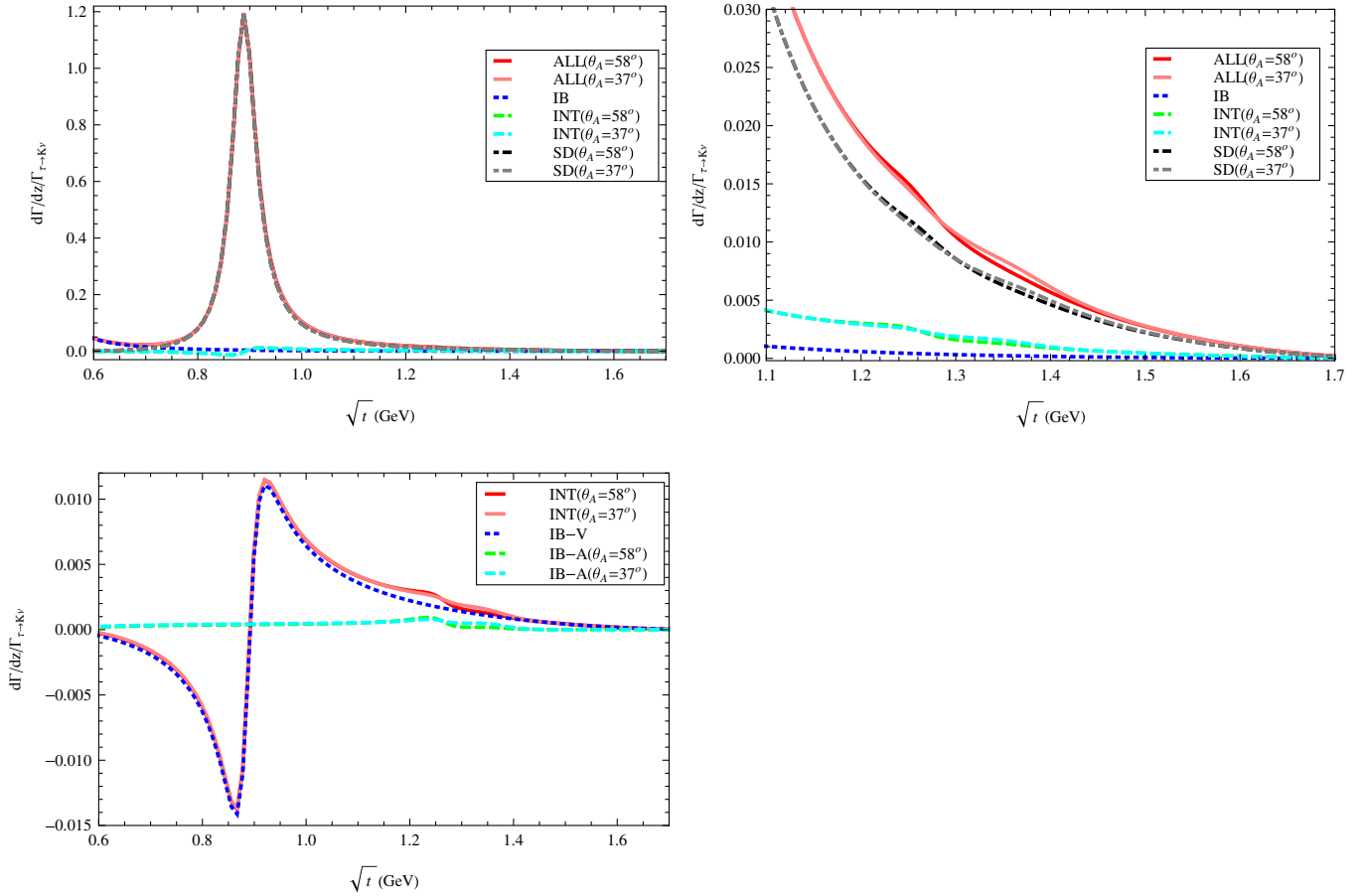
FIG. 13 (color online). Differential decay width (in units of $\Gamma_{\tau \to K\nu_\tau}$) of the process $\tau^- \to K^- \gamma \nu_\tau$, including all contributions as a function of $\sqrt{t}$ with $c_4 = -0.07$. The top right plot is the close-up of the left plot in the region of $\sqrt{t} > 1.1$ GeV. The bottom left plot shows the composition of the interference parts.

the axial-vector neutral resonance with strangeness, $K_{1H,L}$. Since we have not calculated the relevant three-meson decay of the tau, we do not have this expression within $R\chi T$ yet. We took a simple parametrization including the on-shell cuts corresponding to the decay chains $K_{1H,L} \to (\rho K/K^* \pi)$. Since the effect of c_4 is so large, we expect that, once this decay mode is discovered, we will be able to bound this coupling.

As an application of this paper, we are working out [78] the consequences of our study in lepton universality tests through the ratios $\Gamma(\tau^- \to \pi^- \nu_\tau \gamma)/\Gamma(\pi^- \to \mu^- \nu_\mu \gamma)$ and $\Gamma(\tau^- \to K^- \nu_\tau \gamma)/\Gamma(K^- \to \mu^- \nu_\mu \gamma)$ that were considered in Refs. [79–81] in different frameworks. The ratio between the decays in the denominators within χPT was studied in [82,83] and the radiative pion decay has recently been investigated within $R\chi T$ in [36].

ACKNOWLEDGMENTS

APPENDIX A: OFF-SHELL WIDTHS OF THE INTERMEDIATE RESONANCES

The off-shell widths of the resonances used in our numerical discussion are taken from Refs. [10,12,39]. The off-shell width of the $\rho(770)$ is

$$\Gamma_\rho(s) = \frac{sM_\rho}{96\pi F^2}\left[\sigma_{\pi\pi}^3(s) + \frac{1}{2}\sigma_{KK}^3(s)\right], \quad (A1)$$

where

$$\sigma_{PQ}(s) = \frac{1}{s}\sqrt{[s - (m_P + m_Q)^2][s - (m_P - m_Q)^2]}$$
$$\times \theta[s - (m_P + m_Q)^2]. \quad (A2)$$

$\theta(x)$ is the standard unit step function.

The off-shell width of the $K^*(892)$ is

$$\Gamma_{K^*}(s) = \frac{sM_{K^*}}{128\pi F^2}[\sigma_{\pi K}^3(s) + \sigma_{\eta K}^3(s)], \qquad \text{(A3)}$$

while that of the K_{1A} is

$$\Gamma_{K_{1A}}(s) = \Gamma_{K_{1A}}(M_{K_{1A}}^2)\frac{s}{M_{K_{1A}}^2}\left[\frac{\sigma_{K^*\pi}^3(s) + \sigma_{\rho K}^3(s)}{\sigma_{K^*\pi}^3(M_{K_{1A}}^2) + \sigma_{\rho K}^3(M_{K_{1A}}^2)}\right]. \qquad \text{(A4)}$$

The $a_1(1260)$ off-shell width is

$$\Gamma_{a_1}(Q^2) = \Gamma_{a_1}^{3\pi}(Q^2)\theta(Q^2 - 9m_\pi^2)$$
$$+ \Gamma_{a_1}^{KK\pi}(Q^2)\theta(Q^2 - (2m_K + m_\pi)^2), \qquad \text{(A5)}$$

where

$$\Gamma_{a_1}^{3\pi,KK\pi}(Q^2) = \frac{-S}{192(2\pi)^3 F_A^2 M_{a_1}}\left(\frac{M_{a_1}^2}{Q^2} - 1\right)^2$$
$$\times \int dsdt T_{1^+}^{3\pi,KK\pi\mu} T_{1^+\mu}^{3\pi,KK\pi*}. \qquad \text{(A6)}$$

Here $\Gamma_{a_1}^{3\pi}(Q^2)$ recalls the three-pion contributions, and $\Gamma_{a_1}^{KK\pi}(Q^2)$ collects the contributions of the $KK\pi$ channels. In Eq. (A6), the symmetry factor $S = 1/n!$ recalls the case with n identical particles in the final state. The explicit

expressions for $T_{1^+}^{3\pi,KK\pi\mu}$ can be found in Ref. [12]. We stress that the on-shell width, $\Gamma_{a_1}(M_{a_1}^2)$, is a prediction and not a free parameter.

APPENDIX B: NUMERICAL INPUTS

In the numerical discussion, unless a specific statement is given, we use the values given in Ref. [38]. For the pion, kaon, and $K^*(892)$, we use the masses of the charged particles throughout, i.e.,

$$\begin{aligned} m_\pi &= 139.6 \text{ MeV},\\ m_K &= 493.7 \text{ MeV},\\ M_{K^*} &= 891.7 \text{ MeV}. \end{aligned} \qquad \text{(B1)}$$

For the mass of $a_1(1260)$, we use the result of $M_{a_1} = 1120$ MeV from Ref. [12], which has taken the off-shell width effect into account.

For the resonance couplings, once we have the value of the pion decay constant F in the chiral limit, we can determine all of the others except c_4 through Eq. (80). For the value of F, we use $F = 90$ MeV. The physical pion and kaon decay constants we use are

$$F_\pi = 92.4 \text{ MeV}, \qquad F_K = 113.0 \text{ MeV}. \qquad \text{(B2)}$$

[1] H. B. Thacker and J. J. Sakurai, Phys. Lett. **36B**, 103 (1971); R. Fischer, J. Wess, and F. Wagner, Z. Phys. C **3**, 313 (1980); H. K. Kühn and F. Wagner, Nucl. Phys. **B236**, 16 (1984); F. J. Gilman and S. H. Rhie, Phys. Rev. D **31**, 1066 (1985); E. Braaten, R. J. Oakes, and S. M. Tse, Phys. Rev. D **36**, 2188 (1987); A. Pich, Phys. Lett. B **196**, 561 (1987); T. Berger, Z. Phys. C **37**, 95 (1987); N. Isgur, C. Morningstar, and C. Reader, Phys. Rev. D **39**, 1357 (1989); A. Pich, in *Proceedings of the FTUV/89-22 Tau Charm Factory Workshop, Stanford, 1989*, edited by L. V. Beers (SLAC, Menlo Park, California, 1989), p. 416; E. Braaten, R. J. Oakes, and S. M. Tse, Int. J. Mod. Phys. A **5**, 2737 (1990); M. Feindt, Z. Phys. C **48**, 681 (1990); J. J. Gómez-Cadenas, M. C. González-García, and A. Pich, Phys. Rev. D **42**, 3093 (1990).

[2] A. Pich, Nucl. Phys. B, Proc. Suppl. **98**, 385 (2001); M. Davier, A. Hocker, and Z. Zhang, Rev. Mod. Phys. **78**, 1043 (2006); J. Portolés, Nucl. Phys. B, Proc. Suppl. **169**, 3 (2007); A. Pich, Nucl. Phys. B, Proc. Suppl. **181-182**, 300 (2008); G. D. Lafferty, Nucl. Phys. B, Proc. Suppl. **189**, 358 (2009); S. Actis *et al.*, Eur. Phys. J. C **66**, 585 (2010).

[3] R. Decker, E. Mirkes, R. Sauer, and Z. Was, Z. Phys. C **58**, 445 (1993).

[4] R. Decker and M. Finkemeier, Phys. Rev. D **48**, 4203 (1993); **50**, 7079(A) (1994).

[5] C. Q. Geng and C. C. Lih, Phys. Rev. D **68**, 093001 (2003).

[6] J. H. Kühn and A. Santamaría, Z. Phys. C **48**, 445 (1990).

[7] J. H. Kühn and E. Mirkes, Z. Phys. C **56**, 661 (1992); **67**, 364(E) (1995).

[8] D. Gómez Dumm, A. Pich, and J. Portolés, Phys. Rev. D **69**, 073002 (2004).

[9] M. Jamin, A. Pich, and J. Portolés, Phys. Lett. B **640**, 176 (2006); Phys. Lett. B **664**, 78 (2008).

[10] Z. H. Guo, Phys. Rev. D **78**, 033004 (2008).

[11] D. G. Dumm, P. Roig, A. Pich, and J. Portolés, Phys. Rev. D **81**, 034031 (2010).

[12] D. G. Dumm, P. Roig, A. Pich, and J. Portolés, Phys. Lett. B **685**, 158 (2010).

[13] S. Weinberg, Physica (Amsterdam) **96A**, 327 (1979).

[14] J. Gasser and H. Leutwyler, Ann. Phys. (N.Y.) **158**, 142 (1984).

[15] J. Gasser and H. Leutwyler, Nucl. Phys. **B250**, 465 (1985).

[16] J. Gasser and H. Leutwyler, Nucl. Phys. **B250**, 517 (1985).

[17] S. J. Brodsky and G. R. Farrar, Phys. Rev. Lett. **31**, 1153 (1973); Phys. Rev. D **11**, 1309 (1975); G. P. Lepage and S. J. Brodsky, Phys. Rev. D **22**, 2157 (1980).

[18] G. P. Lepage and S. J. Brodsky, Phys. Lett. B **87**, 359 (1979).

[19] H. Albrecht *et al.* (ARGUS Collaboration), Z. Phys. C **33**, 7 (1986).

[20] R. Barate *et al.* (ALEPH Collaboration), Eur. Phys. J. C **4**, 409 (1998).

[21] J. Portolés, Nucl. Phys. B, Proc. Suppl. **98**, 210 (2001).

[22] R. Decker and E. Mirkes, Phys. Rev. D **47**, 4012 (1993); R. Decker, M. Finkemeier, and E. Mirkes, Phys. Rev. D **50**, 6863 (1994).

[23] P. Roig, Nucl. Phys. B, Proc. Suppl. **181-182**, 319 (2008).

[24] S. Jadach, Z. Was, R. Decker, and J. H. Kühn, Comput. Phys. Commun. **76**, 361 (1993).

[25] P. Golonka, B. Kersevan, T. Pierzchala, E. Richter-Was, Z. Was, and M. Worek, Comput. Phys. Commun. **174**, 818 (2006).

[26] G. Colangelo, M. Finkemeier, and R. Urech, Phys. Rev. D **54**, 4403 (1996).

[27] G. 't Hooft, Nucl. Phys. **B72**, 461 (1974); **B75**, 461 (1974); E. Witten, Nucl. Phys. **B160**, 57 (1979).

[28] G. Ecker, J. Gasser, A. Pich, and E. de Rafael, Nucl. Phys. **B321**, 311 (1989).

[29] J. F. Donoghue, C. Ramírez, and G. Valencia, Phys. Rev. D **39**, 1947 (1989).

[30] S. Peris, M. Perrottet, and E. de Rafael, J. High Energy Phys. 05 (1998) 011; M. Knecht, S. Peris, M. Perrottet, and E. de Rafael, Phys. Rev. Lett. **83**, 5230 (1999); S. Peris, B. Phily, and E. de Rafael, Phys. Rev. Lett. **86**, 14 (2001).

[31] A. Pich, in *The Phenomenology of Large N_C QCD: Tempe, Arizona, 2002*, Proceedings from the Institute for Nuclear Theory Vol. 12, edited by R. F. Lebed (World Scientific, Singapore, 2002), p. 239.

[32] B. Moussallam, Phys. Rev. D **51**, 4939 (1995); Nucl. Phys. **B504**, 381 (1997).

[33] M. Knecht and A. Nyffeler, Eur. Phys. J. C **21**, 659 (2001).

[34] P. D. Ruiz-Femenía, A. Pich, and J. Portolés, J. High Energy Phys. 07 (2003) 003.

[35] V. Cirigliano, G. Ecker, M. Eidemüller, A. Pich, and J. Portolés, Phys. Lett. B **596**, 96 (2004).

[36] V. Mateu and J. Portolés, Eur. Phys. J. C **52**, 325 (2007).

[37] G. Ecker, J. Gasser, H. Leutwyler, A. Pich, and E. de Rafael, Phys. Lett. B **223**, 425 (1989).

[38] C. Amsler *et al.* (Particle Data Group), Phys. Lett. B **667**, 1 (2008).

[39] D. Gómez Dumm, A. Pich, and J. Portolés, Phys. Rev. D **62**, 054014 (2000).

[40] F. Guerrero and A. Pich, Phys. Lett. B **412**, 382 (1997).

[41] J. J. Sanz-Cillero and A. Pich, Eur. Phys. J. C **27**, 587 (2003).

[42] I. Rosell, J. J. Sanz-Cillero, and A. Pich, J. High Energy Phys. 08 (2004) 042.

[43] G. Ecker, Prog. Part. Nucl. Phys. **35**, 1 (1995).

[44] A. Pich, Rep. Prog. Phys. **58**, 563 (1995).

[45] J. Wess and B. Zumino, Phys. Lett. **37B**, 95 (1971).

[46] V. Cirigliano, G. Ecker, M. Eidemüller, R. Kaiser, A. Pich, and J. Portolés, Nucl. Phys. **B753**, 139 (2006).

[47] J. Bijnens, L. Girlanda, and P. Talavera, Eur. Phys. J. C **23**, 539 (2002).

[48] S. R. Coleman, J. Wess, and B. Zumino, Phys. Rev. **177**, 2239 (1969); C. G. Callan, S. R. Coleman, J. Wess, and B. Zumino, Phys. Rev. **177**, 2247 (1969).

[49] M. Jamin, J. A. Oller, and A. Pich, Nucl. Phys. **B587**, 331 (2000); P. Buettiker, S. Descotes-Genon, and B. Moussallam, Eur. Phys. J. C **33**, 409 (2004); M. Jamin, J. A. Oller, and A. Pich, Phys. Rev. D **74**, 074009 (2006); S. Descotes-Genon and B. Moussallam, Eur. Phys. J. C **48**, 553 (2006).

[50] B. Moussallam, Eur. Phys. J. C **53**, 401 (2008).

[51] S. G. Brown and S. A. Bludman, Phys. Rev. **136**, B1160 (1964).

[52] P. de Baenst and J. Pestieau, Nuovo Cimento A **53**, 407 (1968).

[53] E. Bycling and K. Kajantie, *Particle Kinematics* (John Wiley & Sons, New York, 1973).

[54] J. J. Sanz-Cillero, Phys. Rev. D **70**, 094033 (2004).

[55] M. Suzuki, Phys. Rev. D **47**, 1252 (1993).

[56] G. Ecker and C. Zauner, Eur. Phys. J. C **52**, 315 (2007).

[57] S. J. Brodsky and G. P. Lepage, Phys. Rev. D **24**, 1808 (1981).

[58] A. V. Manohar, Phys. Lett. B **244**, 101 (1990).

[59] J. M. Gerard and T. Lahna, Phys. Lett. B **356**, 381 (1995).

[60] J. D. Bjorken, Phys. Rev. **148**, 1467 (1966); K. Johnson and F. E. Low, Prog. Theor. Phys. Suppl. **37**, 74 (1966).

[61] F. G. Cao, T. Huang, and B. Q. Ma, Phys. Rev. D **53**, 6582 (1996).

[62] A. V. Radyushkin and R. Ruskov, Phys. Lett. B **374**, 173 (1996).

[63] Z. H. Guo and J. J. Sanz-Cillero, Phys. Rev. D **79**, 096006 (2009).

[64] P. Roig, in *QCD@WORK 2007: International Workshop on Quantum Chromodynamics: Theory and Experiment*, edited by P. Colangelo *et al.*, AIP Conf. Proc. No. 964 (AIP, New York, 2007), p. 40.

[65] K. Kawarabayashi and M. Suzuki, Phys. Rev. Lett. **16**, 255 (1966).

[66] Riazuddin and Fayyazuddin, Phys. Rev. **147**, 1071 (1966).

[67] Z. H. Guo, J. J. Sanz-Cillero, and H. Q. Zheng, J. High Energy Phys. 06 (2007) 030.

[68] S. Weinberg, Phys. Rev. Lett. **18**, 507 (1967).

[69] H. Y. Cheng, Phys. Rev. D **67**, 094007 (2003).

[70] H. Y. Cheng and K. C. Yang, Phys. Rev. D **76**, 114020 (2007).

[71] T. Kinoshita, J. Math. Phys. (N.Y.) **3**, 650 (1962).

[72] M. E. Peskin and D. V. Schroeder, *An Introduction to Quantum Field Theory* (Addison-Wesley, Reading, MA, 1995), p. 842.

[73] D. Becirevic, B. Haas, and E. Kou, Phys. Lett. B **681**, 257 (2009).

[74] Z. H. Guo and P. Roig, "$\tau^- \to \pi^- \gamma \nu_\tau$ as a Source of Background on the Lepton Flavor Violating Decay $\tau^- \to \mu^- \gamma$," Nucl. Phys. B, Proc. Suppl. (to be published).

[75] K. Ikado *et al.* (Belle Collaboration), Phys. Rev. Lett. **97**, 251802 (2006).

[76] B. Aubert *et al.* (BABAR Collaboration), Phys. Rev. D **76**, 052002 (2007).

[77] B. Aubert *et al.* (BABAR Collaboration), Phys. Rev. D **77**, 011107 (2008).

[78] Z. H. Guo and P. Roig (work in progress).

[79] R. Decker and M. Finkemeier, Phys. Lett. B **316**, 403 (1993); Nucl. Phys. **B438**, 17 (1995); Phys. Lett. B **334**, 199 (1994).

[80] A. Sirlin, Nucl. Phys. **B196**, 83 (1982).

[81] W. J. Marciano and A. Sirlin, Phys. Rev. Lett. **61**, 1815 (1988); **71**, 3629 (1993).

[82] V. Cirigliano and I. Rosell, Phys. Rev. Lett. **99**, 231801 (2007).

[83] V. Cirigliano and I. Rosell, J. High Energy Phys. 10 (2007) 005.